

Master thesis : Mission analysis of the OUFTI-Next nanosat

Auteur : Besora Solé, Arnau

Promoteur(s) : Kerschen, Gaetan

Faculté : Faculté des Sciences appliquées

Diplôme : Cours supplémentaires destinés aux étudiants d'échange (Erasmus, ...)

Année académique : 2018-2019

URI/URL : <http://hdl.handle.net/2268.2/6467>

Avertissement à l'attention des usagers :

Tous les documents placés en accès ouvert sur le site le site MatheO sont protégés par le droit d'auteur. Conformément aux principes énoncés par la "Budapest Open Access Initiative"(BOAI, 2002), l'utilisateur du site peut lire, télécharger, copier, transmettre, imprimer, chercher ou faire un lien vers le texte intégral de ces documents, les disséquer pour les indexer, s'en servir de données pour un logiciel, ou s'en servir à toute autre fin légale (ou prévue par la réglementation relative au droit d'auteur). Toute utilisation du document à des fins commerciales est strictement interdite.

Par ailleurs, l'utilisateur s'engage à respecter les droits moraux de l'auteur, principalement le droit à l'intégrité de l'oeuvre et le droit de paternité et ce dans toute utilisation que l'utilisateur entreprend. Ainsi, à titre d'exemple, lorsqu'il reproduira un document par extrait ou dans son intégralité, l'utilisateur citera de manière complète les sources telles que mentionnées ci-dessus. Toute utilisation non explicitement autorisée ci-avant (telle que par exemple, la modification du document ou son résumé) nécessite l'autorisation préalable et expresse des auteurs ou de leurs ayants droit.



Mission analysis of the OUFTI-Next nanosatellite

GRADUATION STUDIES CONDUCTED FOR OBTAINING THE MASTER'S DEGREE IN
AEROSPACE ENGINEERING BY ARNAU BESORA SOLÉ

Author:

Arnau BESORA SOLÉ

Promoter:

Prof. Gaëtan KERSCHEN

UNIVERSITY OF LIÈGE
FACULTY OF APPLIED SCIENCES
ACADEMIC YEAR 2018/2019

Abstract

The OUFTI-Next nanosatellite is the third CubeSat project of the University of Liège. It is intended to serve as a technology demonstrator of agricultural field hydric stress detection from low Earth orbit. This project was introduced in 2016 and was initially envisaged as a 3U CubeSat (30 cm × 10 cm × 10 cm) including a Mid-Wave InfraRed camera. However, in the recent past, the goal of upgrading the payload has led to the proposal of enhancing the platform to a 6U CubeSat (30 cm × 20 cm × 10 cm). This Master's thesis has the objective of shedding some light on this concept, including an updated mission analysis and the design of three working 6U configurations for the OUFTI-Next.

Acknowledgements

First of all, I would like to thank professor Gaëtan Kerschen for giving me the opportunity of being part of this project. Being able to work on a real satellite project was the deciding factor that motivated me to leave my country and discover a new culture and many amazing people.

On top of this, I also wish to thank him, as well as professor Serge Habraken and professor Jérôme Loïcq, for their valuable inputs and comments during our meetings. I am also thankful to my project colleagues, who have allowed me to feel accompanied and have always been helpful when I have needed it, and to Colin Dandumont, who gave me valuable insight at the beginning of the project.

I would like to add a very special thank you to Amaia for always being by my side and encouraging me when I need it, and to my brother Jordi, for always making me feel like home.

Finally, I wish to express my huge gratitude to my parents, who have supported me during all the steps of this amazing journey.

Contents

Abstract	i
Acknowledgements	ii
Contents	iii
Acronyms	vi
1 The OUFTI-Next mission	1
1.1 The project	1
1.2 The mission	2
1.3 Enhanced platform	5
1.4 Introduction to the study	8
2 Preliminary configurations	9
2.1 Volume and power estimation	9
2.1.1 Attitude Determination and Control System	9
2.1.2 Communications System	10
2.1.3 On-Board Computer	12
2.1.4 Electrical Power System	13
2.1.5 Power generation	15
2.1.6 Summary	16
2.2 Panel configurations	18
2.2.1 Configurations description	19
2.2.2 Summary	22
3 Mission analysis	24
3.1 Orbit	24
3.1.1 Launch	24
3.1.2 Lifetime	26
3.1.3 Ground station visibility	29
3.1.4 Summary	32
3.2 Acquisition	33

3.3	Communications	34
3.3.1	Frequency bands	34
3.3.2	Data link	35
3.3.3	Data budget	36
3.4	Attitude and position	39
3.4.1	Position determination	39
3.4.2	Attitude determination and control	40
3.5	Power	41
3.5.1	Operational modes	41
3.5.2	Power consumption	43
3.5.3	Power generation	45
3.5.4	Payload power	46
3.5.5	Battery power	47
4	Systems analysis	53
4.1	Attitude and Position	53
4.1.1	ADCS module	53
4.1.2	GNSS receiver	56
4.2	Communications	57
4.2.1	Commands and telemetry	57
4.2.2	Data download	59
4.3	Power	61
4.3.1	EPS module	61
4.3.2	Solar panels	61
4.4	On-Board Computer	63
4.5	Chassis	64
5	Proposed configurations	65
5.1	OUFTI-Next 6S	65
5.1.1	Components	66
5.1.2	Power budget	67
5.2	OUFTI-Next 6M	68
5.2.1	Components	69
5.2.2	Power budget	70
5.3	OUFTI-Next 6L	72
5.3.1	Components	72
5.3.2	Power budget	73
5.4	Summary	75
6	Conclusions	76

Bibliography	78
A Orbit lifetime simulation results	85
B Battery power simulation results	87

Acronyms

ADCS	Attitude Determination and Control System
AOCS	Attitude and Orbit determination and Control System
BP	Battery Pack
CNES	Centre National d'Études Spatiales
COMM	Communications system
COTS	Commercial Off-The-Shelf
EPS	Electrical Power System
ESA	European Space Agency
GLONASS	Globalnaya Navigatsionnaya Sputnikovaya Sistema (Global Navigation Satellite System)
GPS	Global Positioning System
GS	Ground Station
GSD	Ground Sampling Distance
IADC	Inter-Agency Space Debris Coordination Committee
IMU	Inertial Measurement Unit
ISS	International Space Station
JAXA	Japan Aerospace Exploration Agency
LEO	Low Earth Orbit
LMT	Local Mean Time
LST	Local Solar Time
LWIR	Long-Wave InfraRed

MEO	Medium Earth Orbit
MWIR	Mid-Wave InfraRed
OBC	On-Board Computer
OUFTI-Next	Orbital Utility For Thermal Imaging - Next
PCB	Printed Circuit Board
Rx	Receiver
SNR	Signal to Noise Ratio
SRP	Solar Radiation Pressure
SSO	Sun-Synchronous Orbit
STELA	Semi-Analytic Tool for End of Life Analysis
TBD	To Be Determined
TRx	Transceiver
Tx	Transmitter
UHF	Ultra-High Frequency
VHF	Very-High Frequency
VIS	Visible spectrum

Chapter 1

The OUFTI-Next mission

This introduction chapter provides background on the OUFTI projects, the aim of the OUFTI-Next mission, and the enhanced platform under consideration, to understand the purpose of the study and set the requirements to be fulfilled.

1.1 The project

The Orbital Utility For Telecommunication Innovations (OUFTI-1) was the first nanosatellite developed by the University of Liège and the Liège Space Center. It was a 1U CubeSat (10 cm × 10 cm × 10 cm) which was launched in April 2016 within the ESA Fly Your Satellite! program. It was a demonstrator for a telecommunication protocol called D-STAR, which had a short lifetime, as some days after its launch the communications with the satellite were lost.

After this, the development of the OUFTI-2 started. This is a similar satellite, which will be launched in the near future and will test the D-STAR protocol, as well as two other scientific payloads related to radiation shielding and attitude control measurement.

With the second nanosatellite of this institution under way, a third mission was set in motion in 2016: The Orbital Utility for Thermal Imaging - Next (OUFTI-Next). This was initially projected as a 3U CubeSat (30 cm × 10 cm × 10 cm) for remote sensing of hydric stress in agricultural areas.

For this, the mid-wave infra-red (MWIR) band was selected as the approach for detection. The OUFTI-Next is intended to serve as a technology demonstrator, since this kind of detection is yet to be tested on such a small platform. So the mission's objective is to confirm that this kind of detector can yield exploitable data using a constellation of nanosatellites.

During the first year of the mission development, two feasibility studies of the mission were developed [1] [2], giving promising results. Last year, a total of seven studies regarding different parts of the satellite were carried out, including a global mission analysis [3], a study of the cooling system [4], three different solutions for the optics [5] [6] [7], a thermal analysis [8], and a study of the attitude control and determination [9].

After this, the interest of using other bands besides MWIR has been brought up. So this year, the third stage in the mission design is composed of six studies: a study on the optical system [10], three studies around the detector and imaging system [11] [12] [13], an integrated thermal design [14] and the present assessment of the upgrade to a 6U platform.

1.2 The mission

Hydric stress or water stress is an issue that comes up when plants need more water than what is available. It can also be caused by water quality, salinity or extreme temperatures. If it happens for an extended period of time, it has a severe impact on crops [15]. Plants adapt in a molecular level to their environment, with complex mechanisms to conform to hydric stress. These sharply decrease the crop's growth and productivity, in a natural attempt for survival.

When plants enter these stress states, they block natural transpiration through their leaves, which causes a significant rise in their temperature. This increase in temperature follows a daily cycle with its maximum around midday, when solar radiation is at its peak, and extends for some time due to thermal inertia [16]. This window can be characterized from 12:00 to 14:00 LST, approximately, so the aim is to observe the target crops during this period.

The rise in temperature on the leaves is immediate when the crops are under hydric stress, while visible effects on the plant happen when longer periods of time have passed, which is often too late, as growth and productivity are already severely compromised at this point.

For this reason, the OUFTI-Next aims to spot the differences between the surface and the plants temperature, allowing early detection of hydric stress on crops. This can prevent the losses in growth and productivity in time, by targeting irrigation in function of the needs of each crop.

The final objective is to use this data to create new irrigation strategies with the potential of remarkably increasing productivity of agricultural fields, while avoiding the waste of large amounts of fresh water.

Consistently monitoring crops for this purpose requires having daily or almost-daily updates in observations. Previous studies [1] [2] have determined that even though a single satellite can achieve daily recurrence over a target, it isn't enough to provide full coverage of the Earth, and so a constellation of satellites is ultimately needed. The results show that a constellation of 8 satellites at 800km altitude SSO are enough to fulfill this objective.

However, the first step in this direction is the development of a demonstrator satellite, which doesn't aim to achieve full coverage but to provide proof of the feasibility of this kind of observation using a CubeSat.

This demonstrator is the OUFTI-Next, which has been initially projected as a 3U CubeSat using half of its volume for the platform and the other half for the payload, consisting in a single MWIR detector. Figure 1.2.1 shows a proposal for the configuration of the 3U OUFTI-Next satellite.

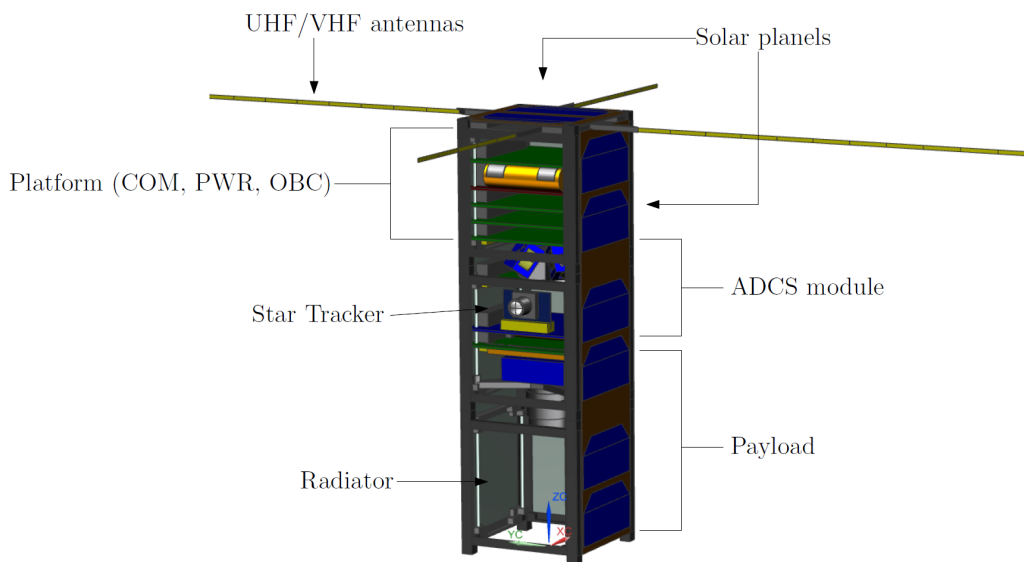


Figure 1.2.1: 3U configuration of the OUFTI-Next satellite [3].

The figure shows that all systems are integrated inside the 3U structure, with the gap for the payload in the lower half of the image. This particular configuration doesn't include deployable solar panels, but some configurations including this option have also been studied in the past.

It is important to remark that all of the past Master's theses that have been referenced revolve around this 3U configuration, and so, all previously drawn conclusions are related to this concept.

Regarding detection, the OUFTI-Next mission is set to use thermal infrared radiation to detect the temperature of the crops. This refers to the infrared spectrum of wavelengths from 3 to 15 μm .

The thermal infrared is split into two bands for observation: the mid-wave infrared (MWIR) from 3 to 5 μm , and the long-wave infrared (LWIR) from 8 to 14 μm . These do not fully cover the thermal infrared spectrum, since the atmosphere is essentially opaque to some specific wavelengths, making them unusable. Figure 1.2.2 shows the transmittance of the Earth's atmosphere as well as the definition of the infrared spectral bands.

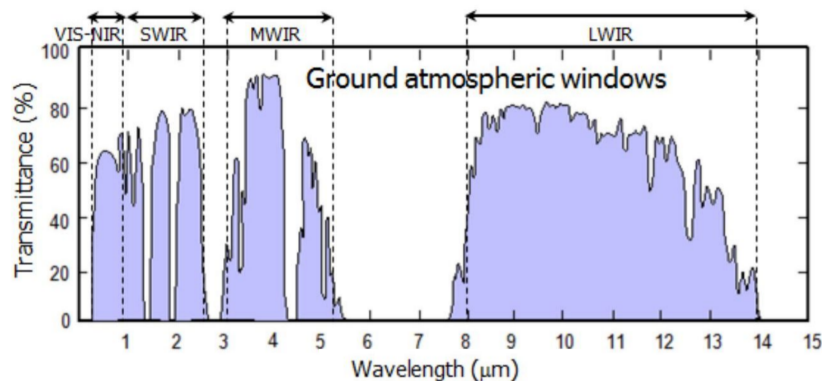


Figure 1.2.2: Infrared spectral bands (extracted from [17]).

The 3U concept of the OUFTI-Next uses the MWIR band for detection, as it presents several advantages over LWIR for being less sensitive to diffraction and disturbances caused by the detector's own radiation. Nonetheless, the detector still needs to be cooled down to avoid this effect, as a detector at ambient temperature won't be able to detect anything besides its own emission.

This kind of detection from space has been done before, although always for larger satellites than the projected OUFTI-Next, and not only using MWIR, as some LWIR solutions also exist [1]. An interesting mission using this technology is Arkyd-6 from Planetary Resources, which is a 6U CubeSat demonstrator for technology intended to detect water resources in space. This mission includes a MWIR detector and was successfully launched in 2018.

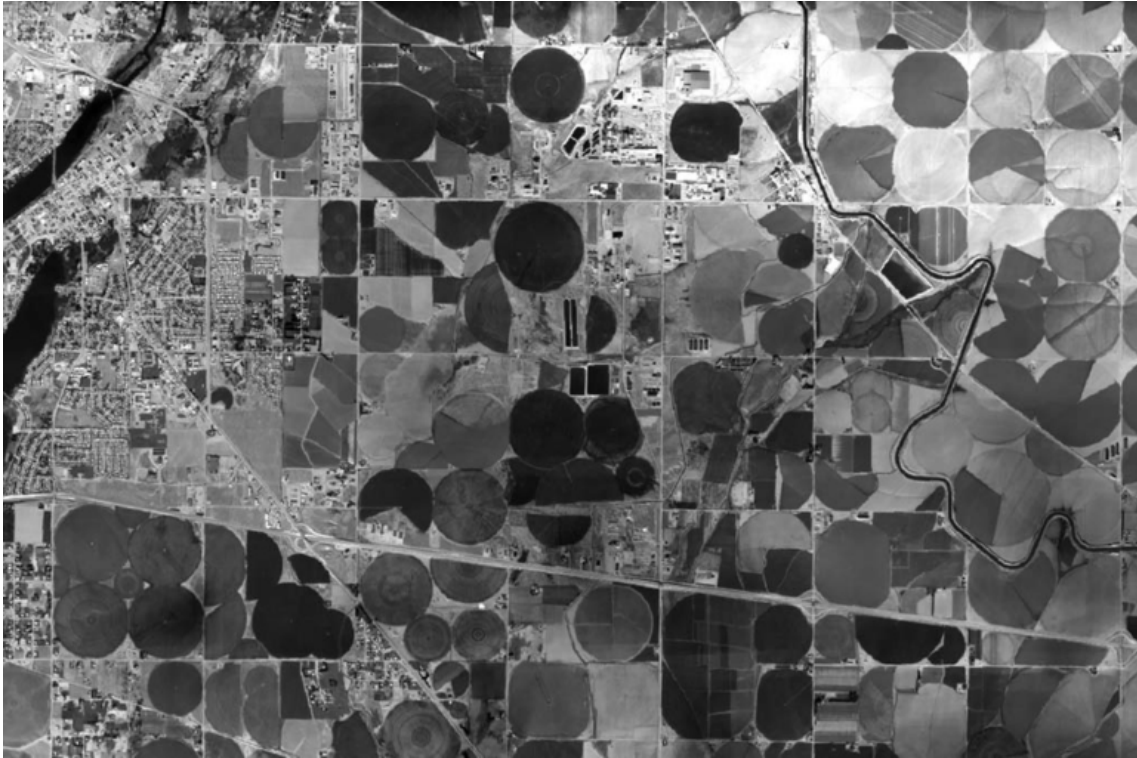


Figure 1.2.3: Agricultural fields detection using MWIR by Arkyd-6 [18].

Besides the MWIR detector, LWIR observation can improve the obtained data by using double-band algorithms. This is usually achieved using dual-band detectors. Also, parallel observation in the VIS spectrum can provide valuable data for target identification, since the raw thermal infrared readings can be hard to identify.

For these reasons, mounting LWIR and VIS detectors besides the main MWIR detector on the OUFTI-Next satellite has been envisaged in the past.

1.3 Enhanced platform

The main problem for including these upgrades in the payload is that the present 3U concept is already tight in volumetric budget. For this reason, an upgrade to a larger platform is proposed. Specifically, the new concept is doubling the size of the satellite, going from 3U (30 cm × 10 cm × 10 cm) to a 6U CubeSat (30 cm × 20 cm × 10 cm).

Besides allowing for the inclusion of a visible spectrum camera, a larger platform also admits an increase in the size of the optics, immediately decreasing diffraction and improving the quality of observations, as well as allowing for simpler optics.

LWIR detectors are more compact than MWIR ones and do not add critical amounts of complexity to the mission, so including this kind of detector in a larger satellite can potentially increase significantly the quality of the observations. The option of a dual-band detector is also possible.

6U CubeSats typically use half of their volume for the platform (3U) and the other half for the payload (3U), as shown Figure 1.3.1, which contains an example of this. However, it is important to remark that this volume distribution and configuration is not the only possible arrangement.



Figure 1.3.1: Example of a 6U CubeSat configuration [19].

This increase in size and payload means that the design of the platform and systems that have been previously sized for the 3U concept needs to be revisited. Since this is an alternative concept for the same mission, the requirements for the 6U configuration are the same as those for the 3U configuration. The ways to achieve these requirements is where the design process diverges.

For the OUFTI-Next demonstrator, the main requirements concern detection. In order to obtain exploitable data about crops, the ground sampling distance (GSD) for the observation needs to be lower than 100 m. However, the target value is set around 50 m.

The requirements on the Attitude Determination and Control System in order to fulfill this imaging resolution without excessive distortion are set to 0.1° in pointing accuracy and 0.5 arcmin/s (or $0.00833^\circ/\text{s}$) for pointing stability. The meaning of these is further discussed in Section 3.4.

Besides, the thermal precision is also key, since it determines the quality of the detection. Values around 1 to 2°C are the requirement for this parameter, as they have been assessed to be feasible [2]. Also, the thermal range of observation is important, and it is set between 0 and 60°C to be able to observe crops in different latitudes and climates.

The 8-satellite constellation is projected to provide full coverage of the Earth every day. The OUFTI-Next demonstrator can not achieve this, so no requirement is set for the full coverage time.

Besides, recurrence can be achieved, but it is not of paramount interest at this stage, so this particular requirement is loosened in order to avoid over-constraining the mission.

The mission lifetime is also key in order to be able to obtain enough data. For this demonstrator, a lifetime over 3 months is considered acceptable. The single updated requirement for this case are the structural limits, which are twice the previous size, a 6U CubeSat, and a maximum of 12 kg [20].

Finally, a summary of the main requirements for the OUFTI-Next demonstrator is displayed in Table 1.3.1.

Volume	6U CubeSat (30 cm×20 cm×10 cm)
Weight	≤ 12 kg
Lifetime	> 3 months
Thermal precision	1 - 2 °C
Thermal range	0 - 60 °C
GSD	< 100 m
Pointing accuracy	0.1°
Pointing stability	0.0083 °/s
Acquisition	A few images a day without a specific target Hour of passage from 12:00 to 14:00 LMT
Payload	TBD

Table 1.3.1: Main requirements for the OUFTI-Next demonstrator.

1.4 Introduction to the study

At this point, the nature of the payload is still to be determined. The number of cameras to be used and the selected detectors are still an open point in the design of the OUFTI-Next satellite.

For this reason, the payload is treated as a black box for the present study, shifting the attention to the 6U platform and aiming to provide some insight into several feasible solutions. With these, during later stages on the mission design of the OUFTI-Next satellite, the appropriate configuration is to be selected depending on the final solution for the payload.

The first part of this study contains a description of the preliminary configurations that have been proposed, mainly concerning the external shape and maximum power characteristics of the satellite.

After this, a mission analysis is presented, including studies performed for each of the proposed configurations. The next chapter contains a detailed analysis of the different systems of the satellite, presenting a sizing and comparison of the components than can be found commercially for each.

This information is then used to go back to the preliminary configurations and present the detailed proposed configurations for the OUFTI-Next satellite, with a discussion of which of them are appropriate for each payload possibility.

Finally, the main ideas and results are summed up in the last chapter, where the drawn conclusions are exposed and the further steps in the design of this concept are outlined.

Chapter 2

Preliminary configurations

This chapter includes a description of the thought process behind the selection of the preliminary configurations for the OUFTI-Next satellite. At this stage, the architecture or specific components are still open, so the satellite is treated as a collection of many black boxes.

2.1 Volume and power estimation

The first step is to gather data of the satellite subsystems to obtain a an estimated volumetric and power budget to use for the projected configurations. For this, a research of COTS modules has been performed to identify a reference volume to assign to each subsystem, as well as a value for its power output or peak power consumption. With this, the volume occupied by the entire platform can be estimated, while the rest of the volume is allocated for the payload, and besides, a global estimation of the power related to the platform can also be done.

2.1.1 Attitude Determination and Control System

Integrated modules for the Attitude Determination and Control System are a simple and accessible solution for CubeSat missions. These systems are independent and widely tested as a unit, so using an integrated module is a much better solution than integrating the ADCS independently, which can provide a more specific solution for the mission's needs, but unnecessarily increases its complexity.

These systems usually provide attitude control by integrating a combination of reaction wheels and magnetorquers. Besides, they use sun sensors, gyroscopes, magnetometers and star trackers to determine the attitude of the satellite.

In a fine-tuned closed loop, the system measures and corrects the attitude of the satellite to provide for the desired pointing in each operational mode.

Table 2.1.1 shows four of these systems that are close to the requirements for the mission. At this stage, their behaviour is not taken into consideration, as this is part of Chapter 4. Rather, only the power and volume of each system is looked at, in order to get an estimation for the volume to allocate for the ADCS, as well as setting the limits for the power consumption of this subsystem.

Company	Model	Volume	Peak power
BlueCanyon	XACT-50	0.75U	2470 mW
CubeSpace	3-Axis ADCS	0.75U	3400 mW
Hyperion	iADCS400	0.67U	4000 mW
KULeuven	KU Leuven ADCS	0.5U	1400 mW

Table 2.1.1: Volume and peak power consumption of COTS ADCS modules.

These four models are specifically designed for 6U CubeSats, so they are all considered applicable at this stage. With this, the drawn conclusion is that ADCS modules for 6U use from 0.5U to 0.75U in volume, and have a peak power consumption between 1 and 4 W.

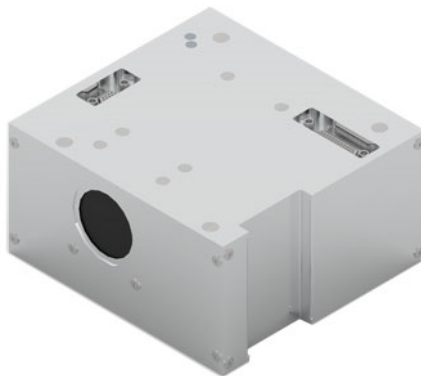


Figure 2.1.1: KU Leuven ADCS module [21].

2.1.2 Communications System

The strategy for communications is yet to be fully defined at this stage. The UHF band is the choice for commands (uplink) and the VHF band is the choice for telemetry (downlink), but the download method of the acquired data is open between VHF, S-band and X-band.

For this reason, similarly to the previous section, a basic research of COTS transmitters, receivers and antennas has been performed. Specifically, of UHF/VHF transceivers (Table 2.1.2), S-band transmitters (Table 2.1.3) and X-band transmitters (Table 2.1.4), with the objective of drawing broad conclusions for each communication strategy.

Company	Model	Volume	Tx power
Endurosat	CubeSat UHF transceiver II	0.1 U	2 W
GOMspace	NanoCom AX100	0.1 U	2.6 W
ISISpace	UHF uplink/VHF downlink transceiver	0.15 U	1.7 W
Nanoavionics	SatCOM UHF	0.1 U	2 W

Table 2.1.2: Volume and power consumption of COTS VHF/UHF transceivers.

An important remark is that, out of the selected VHF/UHF transceivers, the products by Endurosat and Nanoavionics use UHF for downlink as well as uplink. This, however, doesn't set them apart at this stage of design, since their values for power and volume are in the same range as the rest.

With this, VHF/UHF or UHF/UHF commercial transceivers are around 0.1U in volume and 2 W in power consumption during data transmission. So, this is taken as the reference for the power budget.

Company	Model	Volume	Tx power
Clydespace	CPUT S-Band transmitter	0.2 U	5 W
Endurosat	CubeSat S-band transmitter	0.2 U	9 W
GOMspace	NanoCom SR2000	0.1 U	6 W
IQ Wireless	HiSPiCO	0.15 U	5 W
ISISpace	High data rate S-band transmitter	0.33 U	9.2 W

Table 2.1.3: Volume and power consumption of COTS S-band transmitters.

Company	Model	Volume	Tx power
Clydespace	CPUT X-Band transmitter	0.2 U	10 W
Endurosat	X-band transmitter	0.2 U	12 W
IQSpaceCom	XLink	0.3 U	15 W
Syrlinks	EW27	0.25 U	10 W

Table 2.1.4: Volume and power consumption of COTS X-band transmitters.

There are some clear orders of magnitude that can be identified in both S-band and X-band transmitters. All of them take from 0.1U to 0.3U in volume, while there is a clear discrepancy in power consumption: S-band transmitters consume from 5 to 10 W, while X-band transmitters draw from 10 to 15 W. These should be added to the VHF/UHF transceiver values, which are needed either way, to get the total estimation for the communications system.

Adding these up, if VHF is used for downlink, the COMM system needs an approximate volume of 0.1U and around 2 W in power. If the downlink is done by S-band, the volume turns out to be around 0.3U to 0.4U and a power consumption from 7 to 11 W is needed. Finally, for X-band, the volume needed is around 0.3U to 0.4U again, and the power consumption ranges from 12 to 17 W.

For the global analysis, mean values are taken as reference: 0.1U and 2 W for VHF downlink, 0.35U and 9W for S-band, and 0.35U and 14W for X-band communications.



Figure 2.1.2: EnduroSat X-band transmitter module [22].

2.1.3 On-Board Computer

The On-Board Computer system is another of the required systems in the satellite. At this point in design, no specific requirements for memory or processing capabilities are set, so a similar research has been performed, as in the previous sections, with the only requirement of being designed for operation in CubeSats, in order to get reference values for volume and power.

Table 2.1.5 shows the selected OBC systems with their volume and peak power consumption.

Company	Model	Volume	Peak power
CubeSpace	CubeComputer v4.1	0.1 U	435 mW
Endurosat	Onboard Computer (OBC)	0.2 U	440 mW
GOMSpace	NanoMind A3200	0.1 U	900 mW
ISISpace	iOBC	0.12 U	550 mW

Table 2.1.5: Volume and peak power consumption of COTS OBC modules.

For this subsystem, the volume ranges between 0.1 and 0.2U, while the peak power consumption stays under 1W for all considered modules.

It is important to note that the OBC is a cornerstone subsystem in the satellite and, as such, its determination is part of later stages in the design. Nonetheless, the obtained values are a valid reference point for sizing the satellite and allowing a later choice of the most appropriate OBC system.

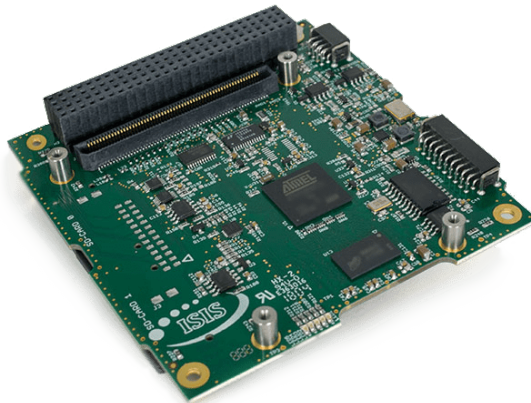


Figure 2.1.3: ISISpace Onboard Computer [23].

2.1.4 Electrical Power System

Finally, the satellite's Electrical Power System can also be obtained commercially to reduce the overall complexity of the platform. Some companies offer ready-made EPS modules that include battery packs. This reduces the overall size and increases simplicity within the satellite, so this kind of EPS have been included in the research.

It is important to note that the size of the EPS, including the battery packs, depends on the power requirements of the satellite. The batteries need to provide enough power to keep the satellite functional during eclipse.

Table 2.1.6 shows the selected EPS modules with their volume and power consumption. Since there can be a wide variety of requirements for this subsystem, very different power systems have been gathered together, for a later classification into groups.

Company	Model	Volume	Power consumption
Crystalspace	P1U Vasik	0.1/0.15 U	15 mW
CubeSatKit	Linear EPS	0.18/0.28 U	100 mW
Endurosat	Power Module I	0.21/0.3 U	75 mW
GOMSpace	NanoPower P31u	0.26 U	160 mW
GOMSpace	NanoPower P60	0.43/0.6 U	600 mW

Table 2.1.6: Volume and power consumption of COTS EPS modules.

Most of the modules allow for two options in battery packs. For this reason, the volume taken by these EPS often takes two values, for a single value of power consumption related to the electronics of the EPS. These are treated separately when classifying the available EPS into groups.

Before that, however, it is interesting to consider the amount of power that can be provided by each battery pack solution. Table 2.1.7 shows the same EPS modules with their volume and power provided by the battery packs.

Company	Model	Volume	Battery capacity
Crystalspace	P1U Vasik	0.1/0.15 U	11/22 Wh
CubeSatKit	Linear EPS	0.18/0.28 U	11/22 Wh
Endurosat	Power Module I	0.21/0.3 U	10.4/20.8 Wh
GOMSpace	NanoPower P31u	0.26 U	20 Wh
GOMSpace	NanoPower P60	0.43/0.6 U	38.5/77 Wh

Table 2.1.7: Volume and battery capacity of COTS EPS modules.

With this information, integrated EPS modules can be split into three groups according to their provided battery capacity: Small EPS modules yielding around 10 Wh in batteries, with volumes between 0.1 and 0.2U and a power consumption between 15 and 100 mW; medium EPS modules providing around 20 Wh of battery capacity, which take from 0.15 to 0.3U and consume from 15 to 160 mW; large EPS modules, with battery capacity values around 40 Wh and power consumption of 600 mW; and finally very large EPS modules, up to around 80 Wh in capacity, 0.6U in volume and 600 mW in power consumption.

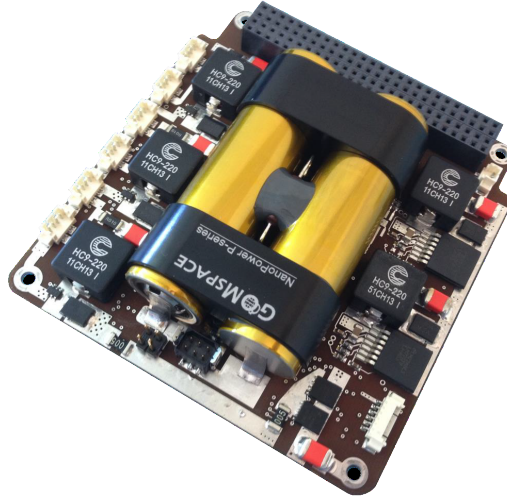


Figure 2.1.4: GOMSpace NanoPower P31u EPS module [24].

In the global configurations, the estimated power demand of each one determine which size of EPS is considered, small, medium or large, for which the mean values are taken. Besides, at this stage, the volume related to antennas is not considered, since they are mounted on the exterior of the satellite and their size doesn't significantly exceed that of a PCB.

2.1.5 Power generation

Solar panels have also been excluded from this volumetric analysis, since they are mounted on the sides of the CubeSat and, if needed, deployed. This means that they are not included in the preliminary volumetric budget, which refers to the interior of the 6U structure. However, their estimated power output is still interesting, so it has been researched. Table 2.1.8 shows the solar panel modules with their estimated power output in LEO.

Company	Size	Efficiency	Power in LEO
EnduroSat	1U	29.5%	2.4 W
EnduroSat	1.5U	29.5%	3.6 W
EnduroSat	3U	29.5%	8.4 W
GOMSpace	1U	30%	2.3 W
GOMSpace	3U	30%	7 W
ISISpace	1U	30%	2.3 W
ISISpace	6U	30%	17 W

Table 2.1.8: Size, efficiency and generated power of COTS solar panels.

Efficiency values for COTS solar panels are around 30%, with an estimated generation of 2.3-2.4W for a 1U panel in LEO. Larger arrays of panels give increased power outputs, since the configurations can be optimized: For 3U, value between 7 and 8.4 W can be achieved, while a single array of 6U can yield up to 17 W in power.

2.1.6 Summary

Taking into account the results obtained for all the relevant subsystems of the satellite platform, the preliminary volumetric and power budgets can be obtained. It is important to bear in mind there are three possible solutions of COMM, depending on the download strategy: VHF, S-band or X-band; and four possible solutions for EPS depending on the power provided by the battery packs: small modules (~ 10 Wh), medium modules (~ 20 Wh), large modules (~ 40 Wh) and very large modules (~ 80 Wh).

The minimum, average and maximum values for each system and option are displayed in Tables 2.1.9 and 2.1.10. With this, some conclusions for the total platform volume and power needed can be drawn, taking the average values obtained from the COTS research.

System	Option	Minimum	Average	Maximum
ADCS	-	0.5 U	0.67 U	0.75 U
COMM	VHF	0.1 U	0.11 U	0.15 U
COMM	S-band	0.2 U	0.3 U	0.48 U
COMM	X-band	0.3 U	0.35 U	0.45 U
OBC	-	0.1 U	0.13 U	0.2 U
EPS	Small	0.1 U	0.16 U	0.21 U
EPS	Medium	0.15 U	0.24 U	0.3 U
EPS	Large	0.43 U	0.43 U	0.43 U
EPS	Very large	0.6 U	0.6 U	0.6 U

Table 2.1.9: Volumetric budget for COTS platform subsystems.

Regarding volume, taking the minimum options (VHF download and small EPS), the platform fits in around 1.1U. This, however, will most likely turn out unfeasible. Opposite from this, taking the maximum options (X-band download and very large EPS), the platform needs 1.75U in total. Taking medium-size options, the total volume for the platform turns out at around 1.4U. This means that the volume that can be dedicated to payload ranges between 4.25 to 4.9 CubeSat units.

System	Option	Minimum	Average	Maximum
ADCS	-	1.4 W	2.8 W	4 W
COMM	VHF	1 W	1.4 W	2 W
COMM	S-band	6 W	8.7 W	11.2 W
COMM	X-band	11 W	13.2 W	17 W
OBC	-	0.4 W	0.6 W	0.9 W
EPS	Small	0.02 W	0.06 W	0.1 W
EPS	Medium	0.02 W	0.08 W	0.16 W
EPS	Large	0.6 W	0.6 W	0.6 W
EPS	Very large	0.6 W	0.6 W	0.6 W

Table 2.1.10: Power budget for COTS platform subsystems.

In terms of power, minimum options require a power consumption of 4.9 W, while maximum options consume up to 17.2 W, on average. Medium-size options for power give an average value for consumption of around 12.5 W. In this case, the communication strategy is the critical aspect that gives this high variation.

In any case, taking into account that eclipse times in the selected altitude range are around 30 minutes, the order of magnitude for battery capacity of medium and large EPS (20 to 40 Wh) is reasonable, keeping in mind the option of very large EPS (80 Wh) if the payload requires such power consumption. This topic is studied in depth in Chapter 3.

Finally, the power generated by the solar panel modules is presented in Table 2.1.11, in a similar fashion to previous results presented in this section.

In this case, in order to compare the different possible arrangements, combinations of smaller modules have been compared with complete modules of the same size. This way, 3 modules of 1U panels yielding 3×2.3 W have been compared to a full 3U module giving 7 W, for example. Like this, the limits and average values for generated power in LEO are obtained.

Size	Minimum	Average	Maximum
1 U	2.3 W	2.3 W	2.4 W
1.5 U	3.4 W	3.5 W	3.6 W
3 U	6.9 W	7.2 W	8.4 W
6 U	13.8 W	14.9 W	17 W

Table 2.1.11: Power generated by COTS solar panels.

2.2 Panel configurations

The second part of this preliminary configuration study is to define the possible external shapes of the satellites, which will be defined by the 6U structure and the deployed systems. If there are any, these can include antennas and solar panels.

However, at this stage, the impact of deployed antennas on the satellite's shape and surface is negligible, so it has been ignored. Thus, the possible solar panel configurations are defined.

In order to provide an estimation for the total power provided by each configuration, reference values obtained in the COTS analysis are used (see section 2.1.6), considering these values are obtained for sun-pointing conditions.

This section contains a description of the proposed configurations, an estimation for the generated power of each one's solar panels, and the values of equivalent surface area, to be used in later calculations of the atmospheric drag effect on the satellite. These values have been obtained using STELA's modeling tool [25].

For reference, the CubeSat's reference X-Y-Z orientation is arbitrarily set with the 6U face normal to the X axis, the 3U face normal to the Y axis, and the 2U face normal to the Z axis. Any other nomenclature is equally valid, yet it is important to have consistency when describing each of the faces and directions. For this study, figure 2.2.1 displays the selected orientation.

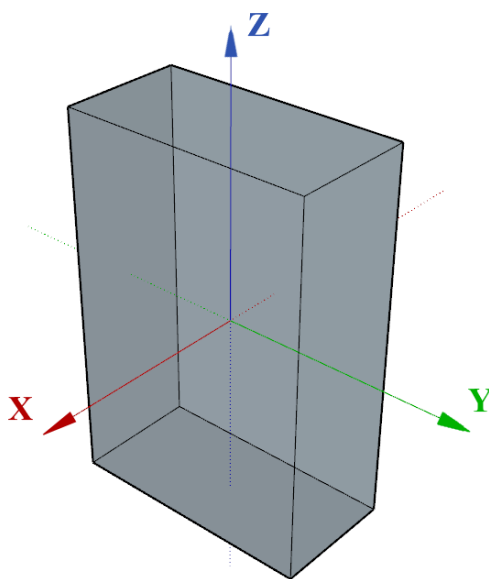


Figure 2.2.1: Selected orientation of the X, Y and Z faces of the CubeSat.

2.2.1 Configurations description

Configuration 1: X face

The first and simplest proposed configuration includes solar panels attached to the X face of the satellite, which means a total panel surface of 6U. One 6U module can be used for optimum power generation up to 17 W.

This configuration includes no hinges, since no deployment of solar panels is required, so the external shape coincides with the 6U prism. For this, the effective surface area is 550.25 cm^2 .

Configuration 2: X, Y and Z face

The second configuration includes solar panels attached to all 3 faces of the satellite, which adds up to a total of 11U of solar panels. One 6U module, one 3U module and two 1U modules can be used in this case.

Adding solar panels on opposite faces is pointless, since they would never generate power at the same time, however, the three faces around one of the satellite's corners can receive solar radiation at the same time, although not perpendicularly. This situation has been optimized using MATLAB, considering the power provided by the solar arrays attached to each face. The optimal orientation for this case is achieved with a rotation of 26.3° around the Z axis, plus a rotation of 14.2° around the resulting Y' axis. This orientation provides an equivalent surface of 7U, which can provide up to 19.6 W.

Regarding the external shape, this configuration is equivalent to Configuration 1, with no hinges and an effective surface area of 550.25 cm^2 .

Configuration 3: X face with sides deployed

The next proposed configuration parts from Configuration 1, adding deployed solar panels from faces +Y and -Y. This gives a flat surface of 12U of solar panels in the X face of the satellite. To achieve this, one 6U module and two 3U modules can be used, giving up to 33.8 W of power.

The effective surface of this configuration is 785.56 cm^2 and it includes two hinges. In the scenario of failure of the deployment mechanisms, power generation of 19 W could be achieved by optimally orienting the satellite 26.3° around the Z axis.

Configuration 4: Z face with sides deployed

Deploying solar panels from faces +X and -X around the top Z face of the satellite creates a flat surface of 14U of solar panels in the Z face. Two 6U modules and two 1U modules can be used for this, yielding up to 38.8 W in total.

This configuration has an effective surface of 1067.24 cm² and includes two hinges. In a deployment mechanism failure scenario, power generation of up to 17.6 W could be obtained by orienting the satellite 15.8° around the Y axis.

Configuration 5: Y face with sides deployed

Similarly to the previous two configurations, deploying solar panels from faces +X and -X around the Y face of the satellite gives a flat solar panel surface of 15U in the Y face. Two 6U modules and one 3U module can be used, providing up to 42.4 W of power.

The effective surface for this configuration is 1029.03 cm², and it also includes two deployment hinges. In the scenario of their failure, the solution would be similar to the one for Configuration 3, achieving a maximum production of 19 W.

Configuration 6: Y face with sides and top deployed

The sixth proposed configuration is similar to the previous one, adding the deployment of the +Z face of the satellite. This adds 2U to achieve a total of 17U of solar panels in the Y face of the satellite. Two 6U modules, one 3U module and two 1U modules are ideally used, generating up to 47.2 W.

For this configuration, the effective surface is equal to 1119.76 cm². This configuration increases the number of hinges to 3. In the worst case of all deployment systems failing, the strategy to follow would be the same as Configuration 2, achieving up to 19.6 W of power.

Configuration 7: All sides deployed at an angle

The concept for the next proposed configuration consists in deploying all sides of the CubeSat, that is faces +X, -X, +Y and -Y. In order to obtain solar power from all of them, they are deployed into a plane extending to both sides of the satellite using four hinges.

Since the satellite isn't axially symmetric around the Z axis, the panels are deployed forming a 154° angle with the X plane, so the panel plane goes through the satellite's geometric center. Otherwise, forces like drag or SRP can considerably impact the satellite's attitude.

A depiction of this configuration is shown in Figure 2.2.2. With this setup, a panel surface of 18U can be achieved, being composed of two 6U modules and two 3U modules. These, in total, can give up to 50.8 W as they can all be positioned facing the Sun.

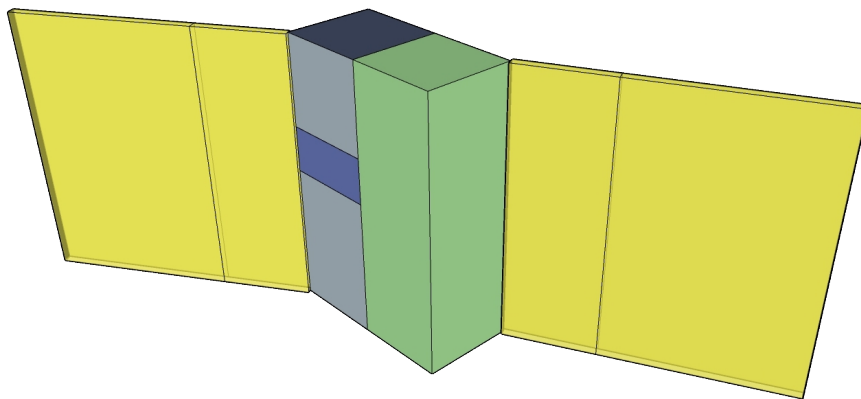


Figure 2.2.2: Basic illustration of Configuration 7.

The effective surface for this configuration is 1405.37 cm^2 . In the scenario of failure of the deployment hinges, the situation would be similar to the failed scenario of Configuration 3, achieving a maximum generation of 19 W. However, in this case, the entire lateral surface of the satellite would be covered, which could block other systems like communications antennas or thermal radiators.

Configuration 8: All sides deployed at an angle plus X and Y faces

For the sake of completion, an eighth configuration is proposed. The concept is similar to configuration 7, adding the front X and Y face to further increase the total power from the solar panels.

In this case, the optimal orientation of the satellite is the same as in the previous configuration, so the panels mounted on faces X and Y don't point directly to the Sun. This means that using three sets of 6U solar panel modules and three sets of 3U panel modules, the maximum power generation that can be achieved is 69.8 W.

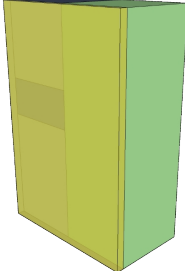
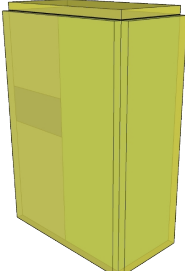
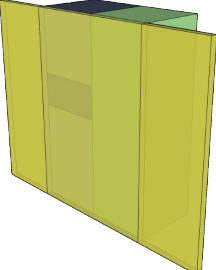
This configuration has the same effective surface and failure scenarios as configuration 7, so this configuration also bears a high risk of interfering with other subsystems in the case of failure of the deployment of the panels.

2.2.2 Summary

Taking into account that the power consumption of the platform can have a value around 12.5 W considering an intermediate solution for communications, none of the configurations are immediately discarded, as they all exceed this amount.

Nevertheless, configurations 1 and 2 are not compatible with the choice of X-band for data download. In this case, the power provided by the solar panels is insufficient.

Finally, as a summary of the proposed preliminary configurations for the satellite, Table 2.2.2 includes the nominal power generated by the solar panels, as well as the achievable power in a deployment fail scenario, in brackets. Besides, the equivalent surface and an illustration are also shown for each configuration.

#	Power	Eq. Surface	Sketch
1	17 W (17 W)	550.25 cm ²	
2	19.6 W (19.6 W)	550.25 cm ²	
3	33.8 W (19 W)	785.56 cm ²	

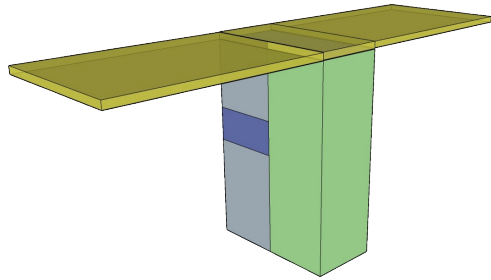
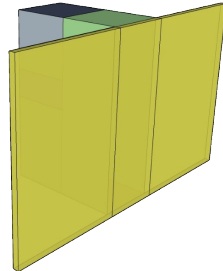
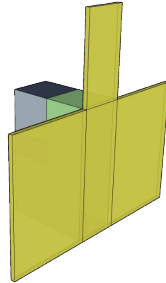
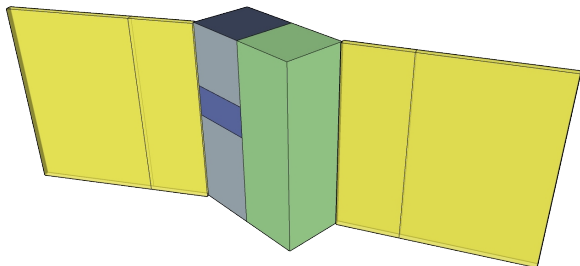
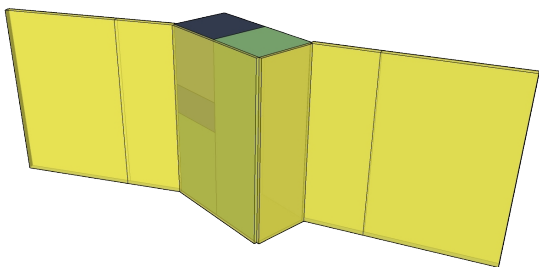
#	Power	Eq. Surface	Sketch
4	38.8 W (17.6 W)	1067.24 cm ²	
5	42.4 W (19 W)	1029.03 cm ²	
6	47.2 W (19.6 W)	1119.76 cm ²	
7	50.8 W (19 W)	1405.37 cm ²	
8	69.8 W (19 W)	1405.37 cm ²	

Table 2.2.2: Preliminary configurations of solar panels.

Chapter 3

Mission analysis

This chapter focuses on the new aspects of the 6U OUFTI-Next mission, not aiming to repeat what has already been studied, but to spot what can be used and what needs updating.

3.1 Orbit

In-depth studies of the considered orbits can be found in previous theses related to the OUFTI-Next 3U configuration [1] [3], and so, the parts that are applicable to a 6U satellite have been used and not replicated. These include crossing times above an area of interest, recurrence over a target on the surface with and without tilting of the satellite, and the duration of eclipse in each of the orbits.

These previous studies are fully applicable to a potential 6U configuration OUFTI-Next mission. However, not all aspects of the orbit analysis are independent from the satellite itself. These points have been studied and are presented in this section.

3.1.1 Launch

One of the key aspects of the development of a satellite mission is the design of a specific orbit that perfectly fits the mission's requirements. For large satellites, this includes a dedicated launch to access this specific orbit. However, CubeSat missions lack the size and budget to make this feasible, so they are usually launched to generic orbits, either in launches dedicated to bringing many small satellites into orbit, or by piggybacking besides a larger satellite.

Either of these concepts allow access to a wide range of target orbits in LEO, two of which have been looked at, in accordance to the mission requirements: Due

to the many launch opportunities and the appropriateness to an Earth observation mission, sun-synchronous orbits have been considered; besides, the ISS orbit has also been looked at because of its high accessibility.

SSO

Sun-synchronous orbits are in a quasi-polar inclination such that the orbit precesses at the same rate as the Earth revolves around the Sun, so it always has the same orientation with respect to it. This means that a satellite in one such orbit passes over any point of the surface at the same local mean solar time throughout the year.

These orbits are widely used for Earth observation missions, since they guarantee the same illumination every day when passing over any given target on the surface, and also for being quasi-polar, so they can observe all latitudes of the Earth.

Launching a 6U CubeSat to sun-synchronous orbit is possible through many options. Three have been considered since they offer periodic launches to a wide variety of altitudes. The first one is ISISpace Launch Services, whose upcoming launches are shown in Table 3.1.1 and range between 450 and 700 km altitude.

Vehicle	Period	SSO Altitude
Russian	H2 2019	450 - 600 km
European	Q4 2019	500 - 700 km
European	Q4 2019	450 - 600 km
USA	Q4 2019	450 - 600 km
Asian	H2 2019	500 - 600 km
Asian	Q3 2019	500 - 600 km
Asian	Q2 2019	500 - 550 km
Asian	Q2 2019	500 - 600 km
European	Q1 2020	500 - 700 km
Russian	H2 2020	500 - 700 km

Table 3.1.1: ISISpace Launch Services upcoming launches to SSO. [26]

Besides, Spaceflight Launch Services [27] also offer several options for accessing SSO in the near future, including many launches between 400 and 650 km, and also up to 730 km altitude.

Finally, RocketLab [28] provide several launches every year to 500km altitude SSO. These set the conveniently accessible altitude range that will be studied for sun-synchronous orbits.

ISS orbit

The ISS orbits Earth at around 400km altitude and an inclination of 51.64° , and there are many opportunities to launch CubeSats from it. However, not all of them allow for 6U configurations. For example, JAXA's JEM Small Satellite Orbital Deployer (J-SSOD) [29] is not compatible with $3U \times 2U \times 1U$ CubeSats, so it's discarded as an eligible deployment option for this configuration of the OUFTI-Next.

The classic NanoRacks CubeSat Deployer (NRCSD) has the same problem, but this company also provides the NRCSD DoubleWide [30], which allows deployments of CubeSats of up to 12U, making it a viable option for deploying on the ISS orbit. Finally, bSpace [31] also offer frequent CubeSat launch and deployment opportunities from the ISS.

3.1.2 Lifetime

The lifetime of an unpropelled nanosatellite in LEO is a key parameter to consider when deciding the target orbit of the mission. An orbit too close to the surface of the Earth will be heavily affected by atmospheric drag which might cause the satellite to re-enter before the completion of the mission.

In opposition, if the satellite is placed at an excessive altitude, the satellite will stay in orbit long after completion of the mission, contributing to the growing issue of space debris. For this reason, IADC guidelines request to dispose LEO satellites such that their orbital lifetime is under 25 years [32].

With this in mind, a range of orbits has been obtained to ensure that the mission is fully completed and also the guidelines set by the IADC are followed. For this reason, the possibility of including an on-board propulsion system to force re-entry from a higher altitude has not been considered.

Simulations for this study have been carried out using STELA [25], a semi-analytic orbit propagator for end of life analysis developed by CNES. This tool uses atmospheric models, solar radiation pressure (SRP), perturbations caused by the Sun and the Moon, as well as Earth zonal perturbations up to 7th order.

The selected atmospheric model is NRLMSISE-00, which is a widely used model for space research. STELA allows to characterize this model with two inputs: The solar activity, quantified by F10.7 solar flux units, and the geomagnetic activity index A_p . The study has been carried out for three different scenarios of solar activity: Maximum (210 sfu), mean (150 sfu) and minimum (75 sfu) [33]. Besides, the selected geomagnetic activity index has been set to 15 as a reference value [34].

STELA simulations have been carried out for configurations 1, 3, 4, 5, 6 and 7 (see Chapter 2), since configurations 2 and 8 have the same equivalent surface as 1 and 7, respectively. The reference surface for each configuration has been calculated using STELA, which allows basic modelling of the satellite configuration to obtain a value for the drag area. The used values for re-entry simulation have been obtained using tumbling mode rather than fixed orientation, since the satellite attitude will not be controlled after the mission is completed and the satellite orbit decays.

The simulation parameters, apart from the reference surface area of the satellite and the atmospheric model, are the following: Mass, which has been set to 12 kg, the maximum value for a 6U CubeSat; the drag coefficient, set to 2.2 as a reference value [35]; the re-entry altitude, set to 120 km as recommended by the software; and the initial orbit. The main parameters of the selected ones are shown in Table 3.1.2.

Orbit type	Altitude	Inclination
ISS [36]	403-408 km	51.6400°
SSO	400 km	97.0305°
SSO	500 km	97.4023°
SSO	600 km	97.7882°
SSO	700 km	98.1886°

Table 3.1.2: Selected orbits for STELA simulation.

Simulation results

Figure 3.1.1 shows the results from all performed simulations in a semi-logarithmic plot. Different line styles indicate values obtained for minimum, mean or maximum solar activity, while different colors indicate each of the configurations of the satellite. In black dashed lines, the limits for the mission have been indicated: An upper limit of 25 years for compliance with the IADC guidelines, and a lower limit of 4 months to guarantee the mission's observation lifetime requirement.

The results show that some configurations decay too quickly for the lowest altitude and maximum solar activity, while the 25-year limit is surpassed in the higher orbits for all configurations, also for mean solar activity.

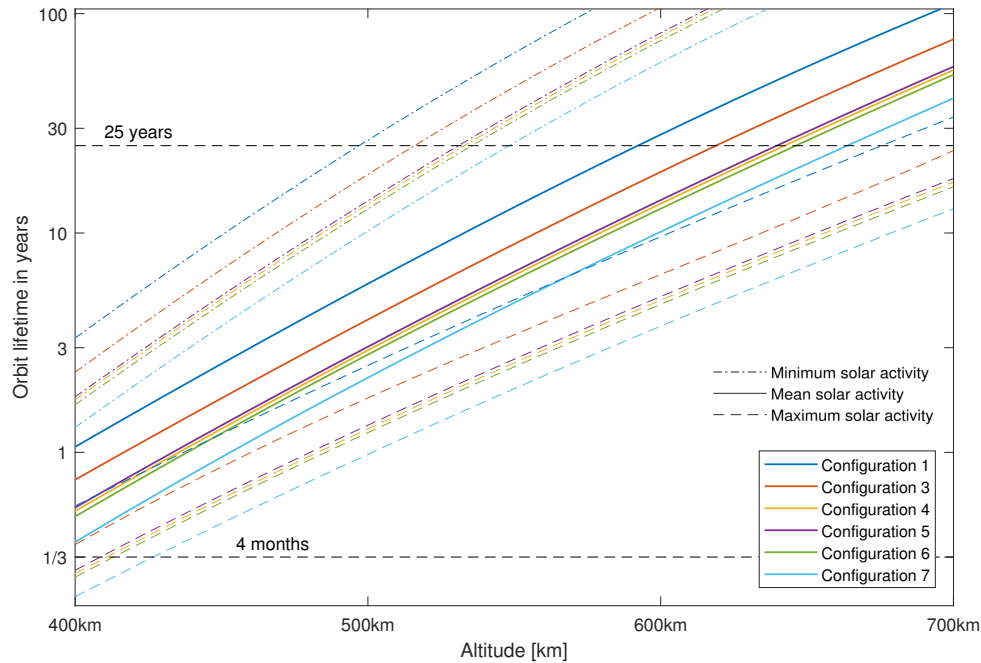


Figure 3.1.1: Orbit lifetime as a function of the altitude for all configurations.

It is also important to note that the mean value for solar activity will match more closely the results that give longer lifetimes, since it follows periodic cycles, while the shorter results are potentially subject to higher variations. This means that values obtained for 25 years of maximum or minimum solar activity are likely unrealistic, while simulations lasting a few months are more sensitive to approaching these limit values.

In order to provide a more visual depiction of the combinations of orbits and configurations that are viable, Table 3.1.3 has been developed. The values in the table are the results for orbit lifetime using mean solar activity, while the colors in the table indicate whether they stay inside the limits for minimum and maximum solar activity.

Green indicates that all simulations (mean, maximum and minimum solar activity) give results between 4 months and 25 years lifetime, which means that configuration and orbit are guaranteed to fulfill both requirements.

Next, values that lie inside the limits for the mean solar activity simulation, but yield more than 25 years for minimum solar activity, or less than 4 months for maximum solar activity, are colored yellow. Finally, red indicates the values that lie outside the required limits for the mean solar activity simulation.

Appendix A contains similar tables with the separate data for all three scenarios of solar activity, which can help further understand the logic behind Table 3.1.3.

	ISS 400km	SSO 400km	SSO 500km	SSO 600km	SSO 700km
Config. 1	1.05	1.06	5.87	28.08	110.89
Config. 3	0.75	0.75	4.03	18.98	76.3
Config. 4	0.53	0.54	2.92	13.59	55.25
Config. 5	0.56	0.56	3.03	14.12	57.33
Config. 6	0.5	0.51	2.79	12.9	52.66
Config. 7	0.39	0.39	2.19	10.13	41.12

Table 3.1.3: Orbit lifetime for mean solar activity, color coded.

The results show that orbits at 400 km might be susceptible to early re-entry in the case of maximum solar activity for the more complex configurations, while the simplest configuration 1 could stay in orbit for too long even at 500 km altitude. All configurations have the potential to stay in orbit more than 25 years at 600km, and they are certain to overtake this limit when placed at 700 km. With this, an adequate orbit is to be selected once the final configuration of the satellite is settled.

3.1.3 Ground station visibility

Increased payload capacity in this version of the OUFTI-Next means that the amount of gathered data is likely to increase as well. This increase needs to be accounted for and foreseen in terms of data budget, but also in terms of communication time. For the orbit analysis, the key point is ground station visibility.

Figure 3.1.2 has been generated with CelestLab and shows the visibility duration for a range of altitudes and maximum elevation angle. This is the maximum angle with respect to the ground that the satellite reaches in a pass, so an elevation angle of 90° means that the satellite passes directly overhead.

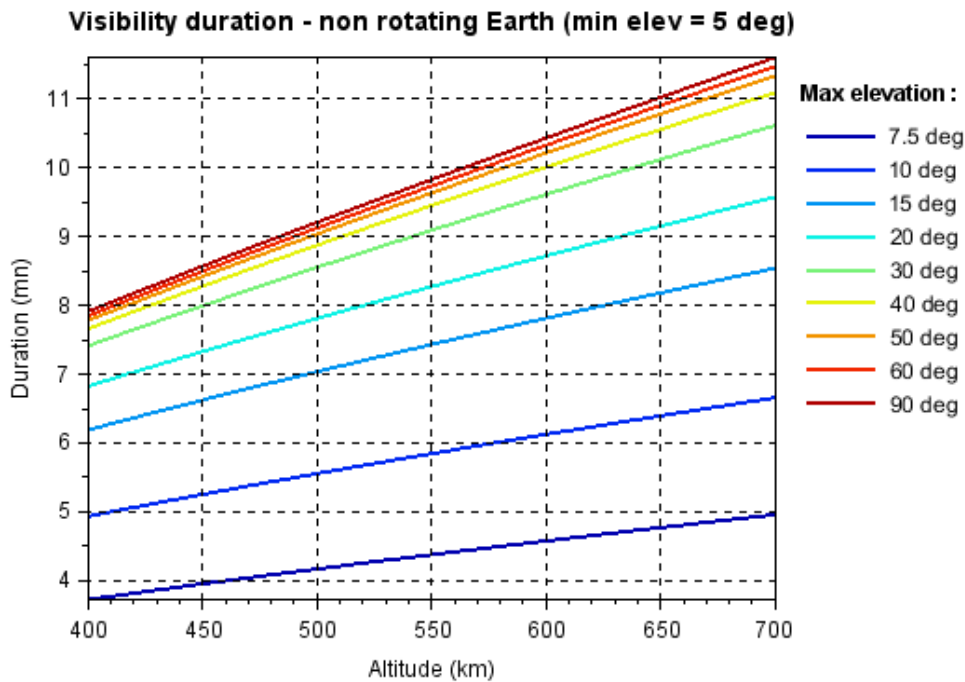


Figure 3.1.2: Visibility duration as a function of the altitude.

For the considered range of altitudes, visibility passes last from 4 to 11 minutes. Note that elevations above 40° are already quite similar to a 90° overhead pass. Taking into account that exploitable passes last for at least 5 minutes [3], passes with maximum elevations of 10° or more are acceptable.

Knowing this, the duration of the visibility passes over the ground station in Liège can be determined and highlighted on the ground track of the satellite. These results have been obtained for the ISS orbit (Figure 3.1.3) and SSO orbits at 400km altitude (Figure 3.1.4), 500km altitude (Figure 3.1.5) and 600km altitude (Figure 3.1.6).

The 700km altitude SSO has been left out of this study after the results obtained in Section 3.1.2, where this orbit failed to fulfill the set requirements in any of the configurations.

Simulations have been run with Celestlab for a total duration of 2 days, which is enough to spot the cycles appearing in visibility passes. Ground tracks, however, are only presented for a duration of 1 day, since it provides a better visualization of the satellite path in each orbit. The visibility passes graphs show the duration and frequency of the passes, including very short passes at a low elevation which are not considered.

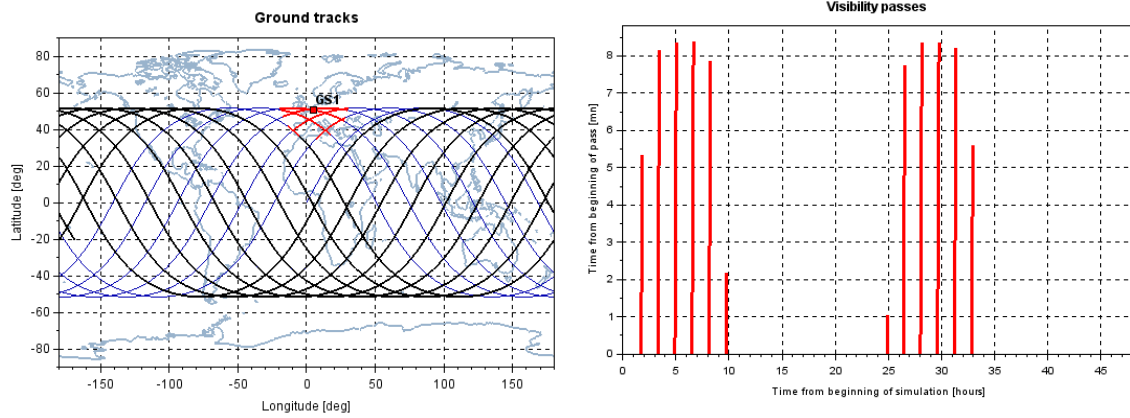


Figure 3.1.3: Ground track (left) and pass duration (right) for ISS orbit.

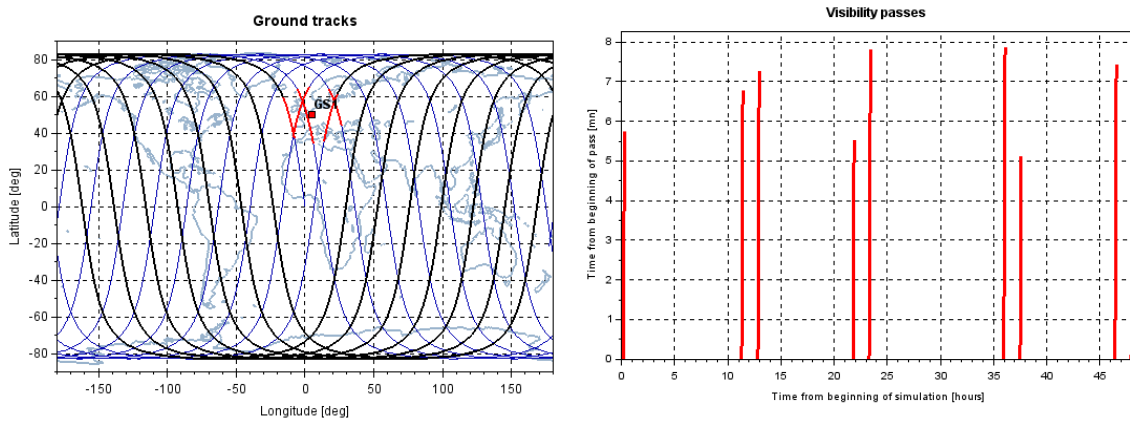


Figure 3.1.4: Ground track (left) and pass duration (right) for 400km SSO.

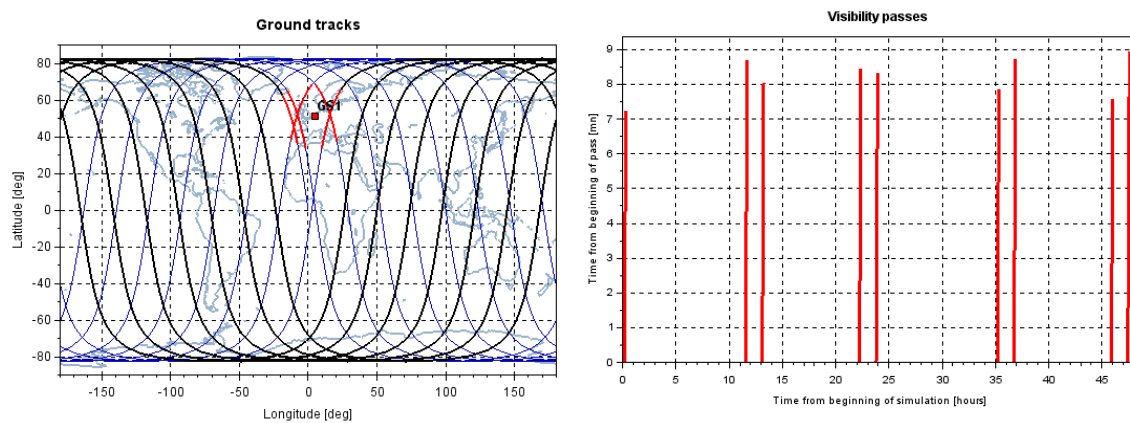


Figure 3.1.5: Ground track (left) and pass duration (right) for 500km SSO.

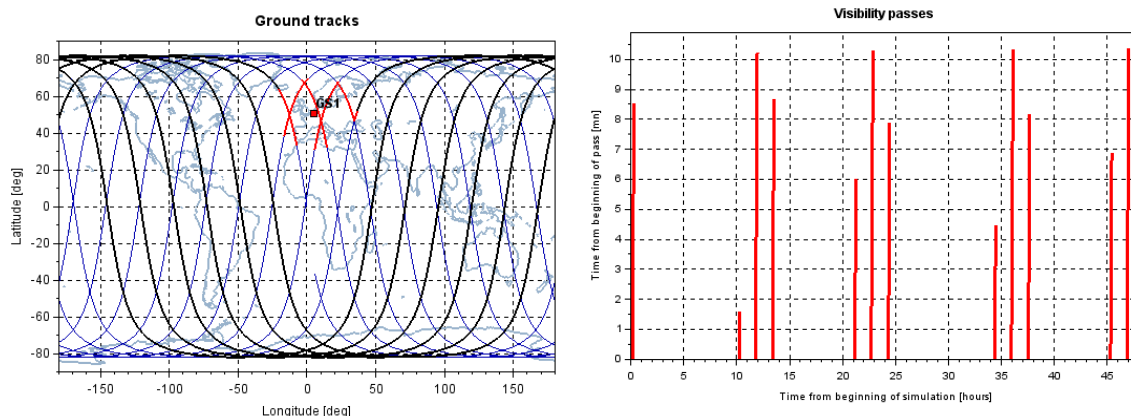


Figure 3.1.6: Ground track (left) and pass duration (right) for 600km SSO.

The ISS orbit is significantly different to the others, with one set of 5 passes per day, lasting from 5 to 8 minutes each. Besides, all considered SSO behave similarly, giving around two sets of 2 consecutive passes per day, with varying duration depending on the altitude. For the lowest of this set of orbits (400km SSO), passes range from 5 to 8 minutes, while the highest (600 km SSO) presents pass times from 8 to 10 minutes.

3.1.4 Summary

The analysis of the orbits shares many aspects with the 3U configurations, but some key differences have been spotted. First, the launch opportunities are more limited but still numerous, providing recurrent access to interesting orbits through diverse means.

Next, the orbital decay time is a critical factor to keep in mind when selecting the final orbit of the satellite, as the configuration of the solar panels can drastically affect the orbit lifetime. SSO above 600 km are advised against, as the satellite might stay in orbit for too long after the mission, while lower orbits around 400 km are susceptible to very short lifetimes. In later stages of the design, an adequate orbit needs to be selected taking into account the information in this chapter.

Finally, regarding the link with the ground station, the results show that across the entire range of considered orbits, the minimum value of 5 minutes of visibility is consistently achieved in every case. Also, all orbits share the value of 4 to 5 visibility passes every day over the ground station in Liège, so these two results can be used in general, as they apply to every orbit in consideration.

3.2 Acquisition

The remote acquisition of the thermal data needed in the OUFTI-Next mission can be done using several strategies: Taking single pictures when the satellite goes over a target; performing a linear scan using either a 1D or a 2D detector; using a time delay integration strategy; or an improved scanning strategy using the AOCS. All of these have been studied previously [2].

The most fitting solution for the OUFTI-Next demonstrator is to take single pictures over specific targets, since there is no need for full Earth coverage at this stage. For this reason, considered detectors contain rectangular arrays of pixels and allow for taking single snapshots. Even with the upgraded payload in a 6U platform, this is the most suitable strategy for the satellite.

The main drawback for most infrared cameras is the required working temperature of the detector. Typical temperatures of 90 K or 150 K, depending on the used technology, are hard to achieve, and require detailed a thermal design of the satellite. This cooling is needed to reduce the SNR down to a point where Earth observation is clear over the noise coming from the emissions of the detector.

This can be solved using several systems, some of which have been studied in the past [3] [4]. These include a full passive system, which has been proven unfeasible; active cooling using a Peltier module, which uses the thermoelectric effect to cool down the detector; and an active cooling system using a cryocooler based on a one-piston Stirling engine to cool down the detector and reject the heat to a radiator. Even though this last solution can negatively affect the satellite's stability due to having moving parts, it has been considered the most promising.

Besides the cooling system, two strategies are possible for cold detection: Either keeping the detector cold permanently, or cooling it down before the detections, and letting it warm back up afterwards. For the active cooling solution using a Stirling engine, cooling the detector before each pass is considered the most viable option.

An alternative to this problematic has been studied in a simultaneous study [11], which introduces the option of using uncooled MWIR and LWIR detectors. These concepts added to a passive solution for cooling the detector though a radiator can be enough to reduce the SNR to usable levels. Nevertheless, this discussion is part of an open argument at this stage in design, and is considered outside of the scope of the present study. The relevant information at this point is the selected acquisition strategy of taking single pictures.

3.3 Communications

The 3U configuration OUFTI-Next is projected to include a payload of one MWIR camera using half of its volume, 1.5U. For this case, the communications budget has arrived to the conclusion that one S-band transmitter is enough to download the data collected by the one MWIR detector [3].

The main target when considering a 6U CubeSat is to increase the total volume dedicated to payload, so that larger or multiple detectors can be used in the same demonstrator satellite. Such an upgrade carries a significant increase in the amount of data that needs to be downloaded from the satellite to the ground station. This chapter contains an assessment of this issue.

3.3.1 Frequency bands

The strategy for basic communications between the ground station and the satellite has been defined in previous stages of the mission as using the UHF band (between 300 MHz and 3 GHz) for sending commands from ground to the satellite, and the VHF band (between 30 MHz and 300 MHz) for downloading telemetry data from the satellite to the ground [1].

This is a very widely used choice for nanosatellite missions and is independent of the actual size of the satellite, so it is accepted in the present design. Besides, the download of data can be done using several strategies, and this point is dependant on the payload.

Although for the 3U concept of the OUFTI-Next, S-band has been selected as the most fitting frequency band for data download, three strategies are considered in this study. The first considered option is using the same VHF band for data download, on top of telemetry. Aside from this, S-band (from 2 to 4 GHz) and X-band (from 8 to 12 GHz) are also considered.

In Section 2.1.2, information of commercial transmitters for all these bands has been gathered. The exact specifications of each are discussed in depth in Section 4.2. For the present analysis, the reference data rate that can be achieved using each technology is enough.

Among all selected VHF/UHF transceivers, the downlink data rate is 9600 bps, the characteristic value for VHF. Regarding S-band transmitters, values range from 1.6 to 4.3 Mbps, with most values being around 2 Mbps. This is selected as the

characteristic value for S-band transmission. Finally, X-band transmitters give data rates from 25 to 100 Mbps, with 50 Mbps as the most common value, and so, this is the selected characteristic data rate for X-band.

3.3.2 Data link

In Section 3.1.3 the windows for communication between the satellite and the ground station have been determined for each considered orbit. This analysis shows that all orbits pass over Liège from 4 to 5 times a day, with visibility times above 5 minutes in all cases. However, for higher altitudes, pass times are longer so more time for data download is available.

It is important to take into account that data download can't be performed during 100% of the visibility pass time, since the communications between the ground station and the satellite need to be established, so time for satellite confirmation and signal acquisition needs to be accounted for. A reference value for this delay is from 1 to 3 minutes [37]. In the present study, the time for signal acquisition is considered as 2 minutes for all orbits and communication systems.

With this, the amount of data that can be downloaded from each orbit can be calculated for the three considered download frequency bands. For this calculation, average pass times have been used (see Figures 3.1.3 to 3.1.6): 8 minutes for the ISS orbit, 7 minutes for the 400 km altitude SSO, 8 minutes for the 500 km altitude SSO, and 9 minutes for the 600 km altitude SSO. The obtained results for downloadable data in one pass are presented in Table 3.3.1.

	VHF (9600 bps)	S-band (2 Mbps)	X-band (50 Mbps)
ISS orbit	3.38 Mb	720 Mb	18 Gb
400km SSO	2.81 Mb	600 Mb	15 Gb
500km SSO	3.38 Mb	720 Mb	18 Gb
600km SSO	3.94 Mb	840 Mb	21 Gb

Table 3.3.1: Data downlink for an average pass in each orbit and frequency.

Obtained values range from a few Mb for VHF, to hundreds of Mb for S-band, to tens of Gb for X-band. It is important to note, however, that the VHF also needs to be used to download telemetry data, so the effective data download is lower.

3.3.3 Data budget

To get a perception of how much data the previously obtained results are, some detector data is gathered. According to [11], the FLIR Neutrino LC [38] is taken as the reference MWIR detector, and the SCD Bird XGA [39] is taken as the reference LWIR detector. Besides, the GOMSpace Aptina MT9T031 [40] is taken as a reference VIS detector.

The selected MWIR detector has a sensor size of 640×512 pixels, the LWIR detector has an array of 1024×768 pixels, and the VIS detector has 2048×1536 pixels. These values and the color depth of the image define the amount of data for each image.

The color depth is the number of bits used to encode each pixel, and it is usually between 8 (1 byte) and 16 (2 bytes), depending on the detector and the required precision on the image. During the selection of the detector, this value needs to be set such that the requirement of 1-2°C is achieved.

To reduce the amount of data to be downloaded, obtained images can be compressed. Compression ratios of up to 2 can be achieved without losses, which halves the amount of data needed to store one image. Further than this, lossy compressions can go up to 100 in compression rates, compromising image quality for reduced data quantities. This option can be studied once the detectors are selected, keeping in mind that the precision in the downloaded images needs to fulfill the requirements, and that image compression needs to be performed on board, either in the OBC system, or in a dedicated processor. At this stage in the design, however, this option is not considered.

Without compression, the size of one image in kB can be calculated as:

$$S \text{ [kB]} = \frac{N \times M \times B}{8 \times 1024} \quad (3.1)$$

Where $N \times M$ is the detector size in pixels and B is the color depth in bits. These results for the considered color depth values and detectors are shown in Table 3.3.2.

	8 bits	10 bits	12 bits	14 bits	16 bits
MWIR detector	320 kB	400 kB	480 kB	560 kB	640 kB
LWIR detector	767 kB	960 kB	1152 kB	1344 kB	1536 kB
VIS detector	4160 kB	5200 kB	6240 kB	7280 kB	8320 kB

Table 3.3.2: Size of one image depending on the color depth and the detector.

With these, three possible scenarios for the payload are considered: The reference MWIR detector; a combination of the MWIR detector and the LWIR detector; and a solution incorporating the MWIR detector, the LWIR detector and the VIS detector.

Since the VIS detector is used for target identification, an 8-bit (1 byte) color depth encoding is considered enough. For the other two detectors, the 16-bit (2 byte) color depth values are taken, to ensure the thermal precision requirement is fulfilled. These values are overestimated for sizing the platform at this stage, but must be revisited when the satellite's payload systems are defined [2].

Using these assumptions, the payload scenario using one detector needs 640 kB to store one picture, the payload combination of two detectors needs 2176 kB, and the payload scenario combining all three reference detectors gives a size of 6335 kB for each image. These values can be used to calculate the time required to download one image using each of the three reference data rates, for VHF, S-band and X-band.

Table 3.3.3 shows the results for the time required to transmit one image using each of the frequency bands in each of the payload scenarios.

	VHF (9600 bps)	S-band (2 Mbps)	X-band (50 Mbps)
MWIR	533 s	2.56 s	0.10 s
MWIR+LWIR	1813 s	8.70 s	0.35 s
MWIR+LWIR+VIS	5279 s	25.34 s	1.01 s

Table 3.3.3: Time required to transmit one image for each payload combination.

Finally, these values can be combined with Table 3.3.1 to obtain the amount of images that can be downloaded at every pass for each orbit. Taking into account the amount of passes per day, the amount of images that can be downloaded per day in each orbit and frequency band are presented in Tables 3.3.4, 3.3.5 and 3.3.6.

	VHF	S-band	X-band
ISS orbit	0.7	141	3516
400km SSO	0.6	117	2930
500km SSO	0.7	141	3516
600km SSO	0.8	164	4102

Table 3.3.4: Daily downloaded images with a MWIR detector.

	VHF	S-band	X-band
ISS orbit	0.2	41	1034
400km SSO	0.2	34	862
500km SSO	0.2	41	1034
600km SSO	0.2	48	1206

Table 3.3.5: Daily downloaded images with a MWIR and a LWIR detector.

	VHF	S-band	X-band
ISS orbit	0.1	14	355
400km SSO	0.1	12	296
500km SSO	0.1	14	355
600km SSO	0.1	17	414

Table 3.3.6: Daily downloaded images with a MWIR, a LWIR and a VIS detector.

The required download time for an image using VHF is not enough to download one image per pass over the ground station, using any of the proposed payload configurations. For this reason, the option of using the VHF band for the data download as well as for telemetry is discarded.

Besides, the obtained values for S-band and X-band data rates allow the download of different orders of magnitude in number of images per day. Using S-band, the system can transmit from tens of images per day, in the maximum payload option, to more than a hundred images per day, for the single detector payload.

Conversely, using the X-band data rate allows for transmissions from several hundreds to several thousands of daily images, depending on the selected payload combination.

At this point, it is relevant to keep in mind that the OUFTI-Next demonstrator mission does not require to provide coverage of any large area. Instead, a lower amount of daily pictures are enough to prove the performance of the detectors on board. Besides, Section 2.1.2 establishes that using X-band communications sharply increases the power demands on the satellite.

For these reasons, the conclusion is that the X-band is an unnecessarily powerful solution for the satellite, which yields an avoidable increase in the power consumption of the satellite in exchange for a needless download data rate. Thus, S-band is selected as the most fitting frequency band for data download.

3.4 Attitude and position

The attitude and orbit determination and control system (AOCS) is a key part of the satellite, and its operation defines the behaviour of the satellite in the different operational modes.

3.4.1 Position determination

Since the satellite doesn't have a position control system, a precise position determination system is needed to provide telemetry data that, together with the readings from the attitude determination system, allow for propagation of the satellite's position during its operation. This is key for developing the commands for the observations that the satellite needs to perform.

In order to determine the satellite's position, observation from the ground can be performed using Doppler effect detection. However, this solution is out of reach since it would require high diameter antennas for tracking. An alternative, then, is to include a GNSS receiver on the satellite, which provides with constant values of position and velocity, to be in turn downloaded as telemetry data.

During operation, the position of the satellite needs to be precisely known in order to correctly identify the observed areas in the acquired data from the detector. Taking a reference altitude of 600 km and a FOV projection on the order of 3km, the satellite position must be known to about 300m in position, or around 50 ms in time, which can be achieved by commercial GNSS receivers [41].

For this reason, a GNSS receiver is included as an additional component in the satellite's platform. This kind of unit doesn't significantly exceed the size of a PCB, and can receive data from GNSS constellations such as the American GPS, the European Galileo or the Russian GLONASS.

These constellations are placed in MEO at altitudes between 20 000 and 25 000 km, so in much higher orbits than the target LEO for observation. With this in mind, the receiver's position on the satellite platform needs to be such that it has visibility of the GNSS constellations in all operational modes.

This kind of system doesn't carry substantial power requirements for the satellite platform, so the selected course of action is to have it in operation all the time. This way, the maximum amount of telemetry data is gathered, so a more precise propagation of the satellite's trajectory can be performed.

3.4.2 Attitude determination and control

The 6U concept of the OUFTI-Next satellite has the same requirements in terms of pointing accuracy and control as the 3U configuration, but a larger volume and mass, and so, a higher inertia for the ADCS to manage.

Although pointing accuracy is very important in an Earth observation satellite, pointing stability is even more so. This is related to avoiding vibrations and jittering on the satellite, which can compromise the entire detection, and are mostly due moving parts inside the satellite like reaction wheels or active cooling systems like Stirling engines.

In nanosatellites, this issue is more relevant than in larger missions, due to their reduced size and inertia. This means that, with respect to the 3U concept of the OUFTI-Next satellite, the 6U configuration is less susceptible to this issue. Nevertheless, it is still the most demanding requirement.

For this reason, the selection of an ADCS integrated module that is specifically designed for at least 6U CubeSats is necessary. With this, the requirement for pointing accuracy is set at 0.1° [3], which is considered an achievable value after checking the performance features of the selected ADCS modules.

Regarding pointing control, a more constraining value of 0.5 arcmin/s ($0.00833^\circ/\text{s}$) is the set requirement for pointing stability [2]. Section 4.1 of the systems analysis contains a detailed evaluation of the selected commercial ADCS modules, with the aim of narrowing down the options that can fulfill these requirements.

In any case, however, the behaviour of the ADCS needs to be studied in depth in later stages of the mission design, once the payload is fully determined and the entire satellite distribution can be modelled. At that point, a detailed analysis of the system can provide confirmation for the fulfillment of the requirements.

The position of this module inside the structure is also relevant. If the system is placed as close as possible to the satellite's center of mass, it minimizes the moments that it has to provide to control the attitude of the satellite, in turn maximizing the provided pointing accuracy and stability. For this reason, this is a key point to be taken into account when defining the final internal configuration of the OUFTI-Next satellite.

3.5 Power

This section contains an assessment of the power values that can be achieved using the power consumption data of the selected COTS components, as obtained in Section 2.1.6.

Having determined the communications strategy, the analysis of the power consumption of the satellite is simplified. With this, the remaining point for discussion about the platform is the size of the EPS and battery packs. Besides, the satellite's payload remains to be determined, so the attainable power supplied to the payload as a whole is also evaluated.

3.5.1 Operational modes

The first step is to determine the satellite's different operational modes. These are defined as four different scenarios during the satellite's operation, that not only define the required behaviour of the satellite in attitude, but determine which of the active subsystems need to be functional at each point.

Mode 1: Power generation

The first operational mode refers to the generation of solar power using the satellite's panel arrays. So, the satellite enters this mode when it is in illumination conditions, that is, not in eclipse.

Besides, this scenario happens when the satellite is far away from the ground station or any target for observation, so for this, no data acquisition is performed, and there is no communication with the ground.

In this case, the ADCS module is active to keep the satellite is sun pointing orientation, in order to maximize the power output of the solar cells. Besides, since there are no communications, the transceiver and transmitter modules are idle. The GNSS receptor is functional, however, as it has been determined to be operational across all operational modes to gather data for telemetry.

The essential components of the satellite, the OBC and the EPS, are in operation, while the payload is not active. So, in these conditions, there is only the potential power consumption related to the payload's idle mode.

Mode 2: Communications

The second operational mode refers to satellite communications with the ground station. This mode is entered when performing a pass over Liège, as determined in Section 3.1.3, so this scenario has a total duration between 5 and 10 minutes in total.

This can happen either during illumination or eclipse, indistinctly. The times this happens during illumination, some power generation is possible during this phase, although reduced, as the satellite's attitude is not sun-pointing.

In this mode, the ADCS module is active to properly orient the satellite for communications, and the communications modules are in operation, so their power consumption is high. Besides, the GNSS receptor, the OBC and the EPS are functional too. Regarding the payload, it is not active in this case like in the previous one, so only its idle power consumption is potentially present.

Mode 3: Data acquisition

The third operation mode concerns the acquisition of data by the detectors, so in this case, the payload is operational. Since detections are performed in the window between 12:00 and 14:00 LMT, this scenario only takes place during illumination. For this reason, some power generation is possible in this mode, but not the nominal value as the satellite's attitude is not optimized for this.

The payload's power consumption defines the upper limit for the determination of the power budget of the mission, so the power consumption in this mode establishes the maximum value that needs to be provided by the satellite's power system.

Depending on the acquisition strategy and the payload characteristics, the duration of this phase varies. For example, taking a single picture over a target takes less than taking several pictures over a broader area. If a pre-detection cooling strategy is required, this also affects the total time the satellite is in acquisition mode.

Regarding the rest of the systems, the ADCS module needs to be active for correct pointing accuracy and stability, as well as the GNSS receptor, OBC and EPS.

The communication systems are idle in this case, since communication and data acquisition never happen at the same time. Should this be required, one of the two operation modes needs to be selected, since considering the simultaneous operation of the payload and COMM systems would carry an excessive sizing in power.

Mode 4: Idle mode

The last operational mode is entered when none of the previously described conditions are given. This is when the satellite is in eclipse and not above the ground station, so no communications can be performed. Thus, the duration of this mode is lengthy, like the power generation mode.

In this case, no data or solar power acquisition is possible, so the satellite is powered by its battery packs. For this reason, the minimum required power consumption is selected for each system.

The ADCS system is in idle mode, so the attitude of the satellite is not precisely controlled; the communications and payload are also idle, consuming minimum power; while the GNSS receiver, the OBC and the EPS are still operational, as they are across all operational modes.

3.5.2 Power consumption

With the different operational modes well defined for the mission, an estimation of the power budget can be performed. For this, the data from COTS components presented in Section 2.1 is used, although specific modules aren't considered at this point. Instead, working with the average values for power consumption of each subsystem in order to draw broader conclusions about each operational scenario. An in-depth discussion on the most fitting particular units is presented in Chapter 4.

Having discarded the VHF and X-band frequencies for data download, the power consumption of the COMM system is narrowed down to the required power of the VHF/UHF transceiver plus the S-band transmitter. These units need an average of 8.7 W when transmitting in Mode 3 and are turned off in the rest of operational modes.

The OBC and the EPS are operational all the time in all modes. The computer modules have an average consumption of 0.6 W, while the EPS require a power supply ranging from 0.02 to 0.6 W, depending on the selected size of the system. This selection is to be done in accordance with the necessary power capacity of the battery packs: EPS including batteries of around 10 Wh use an average of 0.06 W; for around 20 Wh, the average consumption is 0.08 W; while larger batteries of 40 or 80 Wh require an EPS of 0.6 W. For this power budget, however, an average value of 0.3 W is used.

Regarding the ADCS modules, the average power consumption for these is 2.8 W for full operation and 0.7 W for idle or detumbling phases. However, there is a high variation between the considered units, ranging from 1.4 to 4 W for precise pointing. For this reason, the maximum values of 4 W for precise attitude control modes and 0.9 W for idle mode or detumbling maneuvers are used, which correspond to the power consumption that can be needed during the idle operational mode of the satellite. These maximum values are used in this case because taking lower values might result in sizing the power budget to an unfeasible solution. This way, if the eventually selected ADCS module has lower power requirements, this gain can be accounted for the payload.

Finally, the considered GNSS receiver units present values of power consumption between 120 and 170 mW. Taking this into account, a reference value of 0.15 W is used for this system.

Adding up all these values, the reference power consumption for the satellite's platform is obtained and displayed in Table 3.5.1, for each operational mode. The table is color coded in green for systems in full operation, yellow for idle mode or partial functioning, and orange for non operational systems. It is also important to note that these totals are calculated with characteristic values obtained from the COTS analysis, so they can potentially be reduced.

	Mode 1	Mode 2	Mode 3	Mode 4
ADCS Module	4000 mW	4000 mW	4000 mW	900 mW
GNSS Rx	150 mW	150 mW	150 mW	150 mW
VHF/UHF COMM	-	1400 mW	-	-
S-band COMM	-	7300 mW	-	-
EPS	300 mW	300 mW	300 mW	300 mW
OBC	600 mW	600 mW	600 mW	600 mW
Platform Total	5050 mW	13 750 mW	5050 mW	1950 mW
Payload	Idle	Idle	Active	Idle

Table 3.5.1: Power consumption for Mode 1 (Power generation), Mode 2 (Communication), Mode 3 (Acquisition) and Mode 4 (Idle).

3.5.3 Power generation

The maximum power that can be generated by the solar panels depends on each of the proposed configurations in Chapter 2. However, this is only true when the satellite's attitude is such that arrays are optimally facing the Sun in the power generation operational mode.

During the idle mode, the spacecraft is in eclipse, so there is no power generation in this case. Finally, the satellite's attitude for communications and acquisition modes can be characterised as nadir pointing.

With this, simulations for each considered orbit have been performed with Simu-CIC [42] over two days to estimate the average amount of power generated by each configuration, in each orientation (Sun pointing or nadir pointing). The orbit altitude influences the results on the total illumination time, but not the generated power, so this parameter is not used at this point.

The attitude law, however, does affect the Sun angle of the solar arrays. An example of the evolution of this parameter over a 1-day simulation with Sun pointing and nadir pointing is shown in Figure 3.5.1.

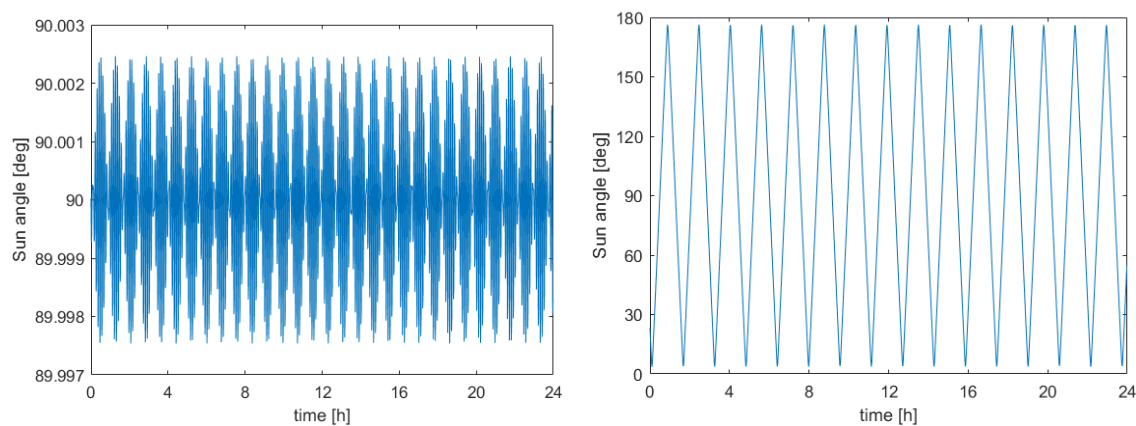


Figure 3.5.1: Evolution of the Sun angle for configuration 1 at a 500km SSO, for sun pointing (left) and nadir pointing (right) attitude.

As expected, the sun-pointing simulation keeps the Sun angle close to normal to the panel plane, maintaining nominal power generation. When keeping the satellite pointing to nadir, the position of the solar panels on the satellite becomes relevant, having high oscillations for panels mounted on side faces, but lower oscillations for panels mounted on the top face. These results can be used to calculate the evolution of the power generation of each configuration over the simulated period.

The power generated by a solar array can be expressed as:

$$P = \mu A G_{SC} V \sin \alpha \quad (3.2)$$

Where μ is the efficiency of the panel, A is its surface area, $G_{SC} = 1361 \text{ W/m}^2$ is the solar constant, V is the Sun visibility (from 0 to 1), and α is the Sun angle, defined as the angle between the Sun direction and the panel plane. With this, the average power generated by every configuration in sun-pointing conditions and in nadir-pointing conditions, during illumination, is shown in Table 3.5.2.

Configuration	Sun pointing	Nadir pointing
1	17.00 W	10.84 W
2	19.60 W	12.51 W
3	33.80 W	21.55 W
4	38.80 W	37.64 W
5	42.40 W	27.34 W
6	47.20 W	30.44 W
7	50.80 W	32.43 W
8	69.80 W	45.79 W

Table 3.5.2: Average generated power for Sun and nadir pointing.

3.5.4 Payload power

With the generated power and the platform consumption, the leftover power for the payload can be characterized. Table 3.5.3 shows the difference between generated power and platform consumption in each configuration and operational mode.

Config.	Mode 1	Mode 2 (ill)	Mode 2 (ec)	Mode 3	Mode 4
1	8.55 W	-5.08 W	-13.75 W	3.62 W	-1.95 W
2	10.63 W	-3.74 W	-13.75 W	4.96 W	-1.95 W
3	21.99 W	3.49 W	-13.75 W	12.19 W	-1.95 W
4	25.99 W	16.36 W	-13.75 W	25.06 W	-1.95 W
5	28.87 W	8.12 W	-13.75 W	16.82 W	-1.95 W
6	32.71 W	10.60 W	-13.75 W	19.30 W	-1.95 W
7	35.59 W	12.19 W	-13.75 W	20.89 W	-1.95 W
8	50.79 W	22.88 W	-13.75 W	31.58 W	-1.95 W

Table 3.5.3: Generated power minus platform consumption in each mode.

For this, a power margin of 20% has been considered in all cases, meaning that the total power consumption can amount to a maximum of 80% of the total power production for each mode. Also, mode 2 has been split into illumination and eclipse, since communications are potentially feasible in both cases.

The negative values in the table indicate that the generated power is less than the required amount only for the platform. In these cases, electrical power needs to be drawn from the batteries.

This means that configurations 1, 2, and maybe 3, depending on the payload's idle power consumption, need to draw power from the batteries for performing communications during illumination. This can potentially be a problem, since battery power is intended and sized for sustaining the systems during eclipse, and eventually for acquisition.

The most critical scenario for this, aside from the unlikely case that the idle consumption of the payload exceeds 12 W, is the scenario where communications are performed during eclipse. In this case, the batteries need to provide an estimated 13.75 W plus the idle consumption of the payload, during the time for the communications pass. This scenario sets the limit for the maximum idle power consumption of the payload, in relation to the battery capacity.

Besides, the payload is only active in mode 3, so the maximum operational power consumption that the payload can have, without relying on battery power, is defined by the mode 3 column of Table 3.5.3. This value ranges from 3.6 to 32.6 W, which means that the proposed satellite configurations allow for a wide variety of on-board payloads. The precise values, however, can differ greatly, since the power generation during acquisition is not granted. For this reason, the batteries must be able to provide enough power for the payload, regardless of generation.

3.5.5 Battery power

The maximum power output of the battery pack depends directly on the payload. As has been stated in the previous section, the necessary battery power output is determined by the payload's operational consumption.

Regarding the battery capacity (Wh), the required values depend on the amount of time spent on each operational mode. For this assessment, four reference scenarios are considered:

- Scenario 1: A simple orbit with no events. Sun-pointing attitude and operational mode 1 during illumination, and mode 4 during eclipse.
- Scenario 2: An orbit with a communication pass during illumination. Sun-pointing mode 1 during most of the illumination time, except for a nadir-pointing pass with duration depending on each orbit (see Section 3.1.3), plus mode 4 during eclipse.
- Scenario 3: An orbit with a communication pass during eclipse. Similar to the previous scenario with different total times.
- Scenario 4: An orbit with an observation pass. Similar to scenario 2, with mode 3 during acquisition, which is considered to last for 10 minutes.

Table 3.5.4 shows the characteristic time periods of each orbit, including the typical communication pass time over the ground station. Maximum values are used for the eclipse times.

	ISS orbit	400km SSO	500km SSO	600km SSO
Illumination	56 min 13 s	56 min 24 s	58 min 48 s	61 min 09 s
COMM pass	8 min 00 s	7 min 00 s	8 min 00 s	9 min 00 s
Eclipse	36 min 14 s	36 min 09 s	35 min 48 s	35 min 32 s
Full orbit	92 min 49 s	92 min 33 s	94 min 36 s	96 min 41 s

Table 3.5.4: Characteristic times of illumination, COMM and eclipse for each orbit.

Using these times, it is possible to compute the minimum necessary battery capacity for each configuration and scenario, in each orbit. This evolution has been calculated along each orbit and scenario, selecting the rate of charge or discharge of the batteries according to the power generation or consumption in each case. All eight configurations have been studied in order to form basic ideas about each one's feasibility.

It is important to keep in mind that the life cycle of the batteries lowers their maximum capacity. This decline is a function of the number of cycles and also the depth of discharge, or the lowest percentage reached at every cycle.

According to [41], the life cycle of a typical battery pack in LEO achieves a lifetime of 1 year if the depth of discharge is around 49% at each cycle. Taking into account the requirements for the mission, a maximum depth of discharge of 50% has been used for this study.

Table 3.5.5 contains the minimum required battery capacity for each configuration and scenario, for the ISS orbit and the 400 km altitude SSO. Next, Table 3.5.6 presents the same information for the 500 km and the 600 km altitude SSO.

#	ISS orbit				400km SSO			
	Sc. 1	Sc. 2	Sc. 3	Sc. 4	Sc. 1	Sc. 2	Sc. 3	Sc. 4
1	3.57	5.19	6.71	5.70	3.56	4.98	6.31	5.69
2	3.57	4.83	6.71	5.25	3.56	4.67	6.31	5.24
3	3.57	3.57	6.71	3.57	3.56	3.56	6.31	3.56
4	3.57	3.57	6.71	3.57	3.56	3.56	6.31	3.56
5	3.57	3.57	6.71	3.57	3.56	3.56	6.31	3.56
6	3.57	3.57	6.71	3.57	3.56	3.56	6.31	3.56
7	3.57	3.57	6.71	3.57	3.56	3.56	6.31	3.56
8	3.57	3.57	6.71	3.57	3.56	3.56	6.31	3.56

Table 3.5.5: Required battery capacity for ISS orbit and 400km SSO, using a 10 W payload and a 50% depth of discharge. Values in Wh.

#	500 km SSO				600km SSO			
	Sc. 1	Sc. 2	Sc. 3	Sc. 4	Sc. 1	Sc. 2	Sc. 3	Sc. 4
1	3.53	5.15	6.67	5.65	3.50	5.32	7.04	5.63
2	3.53	4.79	6.67	5.21	3.50	4.95	7.04	5.18
3	3.53	3.53	6.67	3.53	3.50	3.50	7.04	3.50
4	3.53	3.53	6.67	3.53	3.50	3.50	7.04	3.50
5	3.53	3.53	6.67	3.53	3.50	3.50	7.04	3.50
6	3.53	3.53	6.67	3.53	3.50	3.50	7.04	3.50
7	3.53	3.53	6.67	3.53	3.50	3.50	7.04	3.50
8	3.53	3.53	6.67	3.53	3.50	3.50	7.04	3.50

Table 3.5.6: Required battery capacity for 500km and 600km SSO, using a 10 W payload and a 50% depth of discharge. Values in Wh.

Across all orbits and configurations, the limiting requirement for battery capacity corresponds to scenario 3, relative to performing communications with the ground station during eclipse.

The other main conclusion drawn from this study is that the power generation is always enough. Even configuration 1, which has the minimum amount of panels, can power the satellite in all the proposed scenarios.

This gives a minimum battery capacity of 6.71 Wh for the ISS orbit, 6.31 Wh for the 400 km altitude SSO, 6.67 Wh for the 500 km altitude SSO, and 7.04 Wh for the 600 km altitude SSO, whichever the configuration.

These values have been obtained using a value for the payload power consumption of 10 W in operational mode, and 1 W in idle mode. In order for the limiting case to arise for the acquisition scenario, payload operational consumption needs to be over 13 W. For payloads under this power consumption, the required battery capacity is the one stated above.

Besides, the payload's idle power consumption can have values up to 4.7 W so the battery packs can be fully charged again during illumination. This limit can be seen in Figure 3.5.2, which shows the evolution of the battery capacity of Configuration 1 in the ISS orbit along scenario 3, for several values of payload idle power consumption.

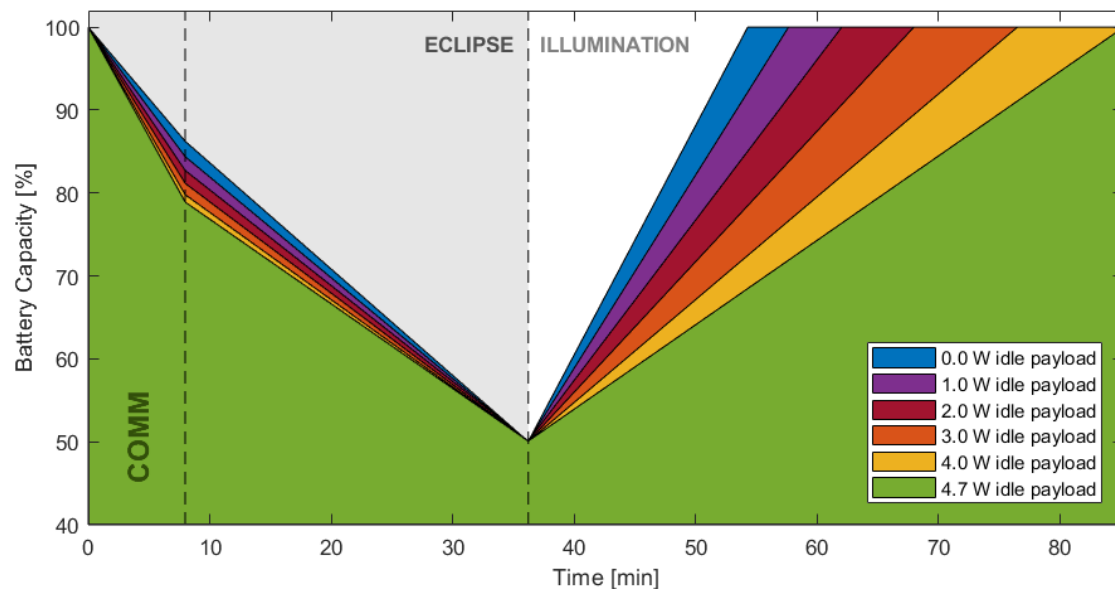


Figure 3.5.2: Battery capacity for Configuration 1 in the ISS orbit and scenario 3.

The detailed values of all the performed simulations can be found in Appendix B.

Next, the same study has been performed for a payload with 20 W of operational power consumption. Since the data acquisition scenario (number 4) is the limiting case, there is no need to show the results for all simulated cases again. So, the minimum battery capacity requirements for scenario 4 and a 20 W payload are shown in Table 3.5.7.

#	ISS orbit	400km SSO	500km SSO	600km SSO
1	9.03	9.02	8.98	8.96
2	8.58	8.57	8.54	8.51
3	6.17	6.16	6.13	6.1
4	3.57	3.56	3.53	3.50
5	4.63	4.62	4.58	4.56
6	3.8	3.79	3.76	3.73
7	3.57	3.56	3.53	3.50
8	3.57	3.56	3.53	3.50

Table 3.5.7: Required battery capacity using a 20 W payload. Values in Wh.

Once again, all panel configurations provide enough power to successfully feed the systems of the satellite in all considered scenarios. As long as the payload's idle power consumption is under 2.8 W, configuration 1 provides enough power generation for this kind of payload. Configuration 2 stops being sufficient when the payload's idle power consumption overtakes 5.1 W. For larger idle consumption values in idle mode, configurations 3 to 8 are suitable.

The main conclusion to be drawn from this is that, in the situations where the payload is limiting, the orbit doesn't have much of an effect on the required battery capacity. For this reason, the same study has been performed for 30 and 40 W payloads, taking the maximum values among the orbits.

The results for minimum battery capacity requirements are displayed in Table 3.5.8 for all the considered generic payloads: 10 W, 20 W, 30 W and 40 W of total operational power consumption. Besides, Table 3.5.9 contains the maximum idle power consumption that each configuration can hold, for each payload case.

#	10W Payload	20W Payload	30W Payload	40W Payload
1	7.04	9.03	12.36	15.69
2	7.04	8.58	11.92	15.25
3	7.04	6.17	9.5	12.84
4	7.04	3.57	5.21	8.55
5	7.04	4.63	7.96	11.29
6	7.04	3.80	7.13	10.47
7	7.04	3.57	6.60	9.94
8	7.04	3.57	3.57	6.37

Table 3.5.8: Required battery capacity for generic payloads. Values in Wh.

#	10W Payload	20W Payload	30W Payload	40W Payload
1	4.8	2.6	0.5	-
2	7.3	5.0	2.8	0.7
3	10.0	18.0	15.8	13.6
4	10.0	20.0	22.6	20.4
5	10.0	20.0	23.7	21.5
6	10.0	20.0	28.0	25.9
7	10.0	20.0	30.0	29.1
8	10.0	20.0	30.0	40.0

Table 3.5.9: Maximum supported idle power for generic payloads. Values in W.

The results indicate that in the case of using deployable solar panels, mounting them on the top face of the satellite (+Z) helps increase the power consumption during nadir pointing, and so, lowers the requirements for the battery packs.

Nevertheless, if the payload's power consumption in idle mode is low, the simplest configurations appear to be enough to power the satellite, making deployable panels not necessary in such cases.

Chapter 4

Systems analysis

Having analysed the mission and narrowed down its requirements using generic values for each subsystem, the next step is to consider the specific units to be incorporated in the platform. This chapter contains a detailed analysis of the modules introduced in Chapter 2, in order to select the most fitting for the OUFTI-Next demonstrator.

4.1 Attitude and Position

The first platform subsystem to be assessed is the Attitude and Orbit Determination and Control System. For this mission, it consists of an integrated ADCS module and a GNSS receiver.

4.1.1 ADCS module

Four integrated ADCS modules have been considered for the 6U platform: The Blue Canyon XACT-50, which is an upgraded version of the widely used XACT-15 including larger reaction wheels and magnetorquers to adapt the module to larger platforms; the CubeSpace 3-Axis CubeADCS; the Hyperion iADCS400, a larger version of the previously considered iADCS100; and the KULeuven ADCS, developed at the KUL university in Belgium.

Table 4.1.1 shows the main characteristics of all four modules, including the operational requirements for pointing accuracy and stability, power consumption and information about each unit's flight heritage. Unfortunately, some information is missing, although not critical values. The information in Table 4.1.1 has been obtained from [43], [44], [45], [46], [47], [48], [49], [50], [3] and [21].

Company	Blue Canyon Technologies	CubeSpace	Hyperion Technologies	KU Leuven
Name	XACT-50	3-Axis CubeADCS	iADCS400	KU Leuven ADCS
Volume	0.75U	0.75U	0.67U	0.5U
Mass	1230 g	1300 g	1150 g	715 g
Sensors	IMU (Gyroscopes) Magnetometer Sun sensor Star tracker	Gyroscopes Magnetometer Sun sensor Star tracker	Gyroscope Star tracker	3 Gyroscopes 6 Photodiodes 3 Magnetometers Star Tracker
Actuators	3 Reaction wheels 3 Magnetorquers	3 Reaction wheels 2 Ferrite core torquers 1 Air core coil	3 Reaction wheels 3 Magnetorquers	3 Reaction wheels 3 Magnetorquers
Momentum storage	50 mN m s	30 mN m s	30 mN m s	4 mN m s
Torque	7 mN m	2.3 mN m	2 mN m	0.5 mN m
Pointing accuracy¹	<0.003°	<0.06°	<<1°	<0.01°
Pointing stability¹	<0.003°/s	<0.1°/s	-	-
Slewing rate¹	≥10°/s	-	>1.5°/s	-
Operating temp.	-30 °C to 50 °C	-10 °C to 70 °C	-45 °C to 85 °C	-
Peak Power	2470 mW	3400 mW	6000 mW	1400 mW
Idle Power	500 mW	760 mW	900 mW	940 mW
Flight heritage	Since 2016 for XACT (2019 for XACT-50)	Since 2014 (Except star tracker)	Since 2017 for iADCS100	-
Cost	\$125 000	\$58 000	\$75 000	-

Table 4.1.1: Characteristics of the considered ADCS modules.

¹Reference values for similar missions.

Considering the momentum storage capabilities of the three first units, specifically designed for controlling 6U missions, the KULeuven ADCS module is significantly lower in this aspect. Its maximum torque is also one order of magnitude below the rest.

Even though the KULeuven ADCS manufacturer claims that this module is enough to control satellites up to 12U, comparison with the modules that have been used in the past for missions this size indicates that this might not be enough.

Once the payload of the satellite is defined, a detailed analysis of this module needs to be performed, including simulations to verify whether it is sufficient. If it is, it is better than the rest in mass, volume and power consumption, even though it hasn't had any flight heritage at the moment.

Besides this unit, the other three have similar weight, size and momentum capabilities. All of them have some flight heritage, at least for very similar smaller units, in past successful satellite missions. Besides, all of them can fulfill the mission's requirement for pointing accuracy.

Regarding pointing stability, the XACT-50 has achieved values fulfilling the mission's requirement in previous similar satellites [45], while the CubeADCS has achieved values near the missions requirements [3]. No information about this has been found for the iADCS400, however.

The iADCS400 also has a significantly higher power consumption than the rest, so it is discarded for this reason. This leaves the XACT-50 as the most fitting unit for the demonstrator, with low power consumption, plenty of flight heritage and definitely fulfilling the requirements in pointing accuracy and stability.



Figure 4.1.1: Blue Canyon XACT-50 ADCS module [43].

The only drawback for the XACT-50 is its cost, being significantly higher than the rest. The 3-Axis CubeADCS is the next best option, with slightly higher power consumption and less flight heritage, but coming close to the mission's requirements.

4.1.2 GNSS receiver

Next, the choice in GNSS receivers is assessed. Four units have been considered: The Hyperion GNSS200, the SkyFoxLabs piNAV-NG, the NovAtel OEM719 and the NewSpace NSS GPS Receiver. All of them are intended to provide position determination for nanosatellite missions.

Company	Hyperion	SkyFoxLabs	NewSpace	NovAtel
Name	GNSS200	piNAV-NG	NSS GPS Rx	OEM719
Volume [mm]	20×15×3	75×35×12.5	96×96×15	46×71×11
Mass	3 g	24 g	110 g	31 g
Power	150 mW	125 mW	1 W	1.8 W
Tracking rate	10 Hz	1 Hz	1 Hz	100 Hz
Constellations	Multiple	GPS	GPS	GPS/GLONASS
Pos. accuracy	8 m	10 m	10 m	1.5 m
Vel. accuracy	-	0.10 m/s	0.25 m/s	0.03 m/s
Temperature	-45 to 85 °C	-40 to 85 °C	10 to 50 °C	-40 to 85 °C
Cost	-	\$6900	-	\$7950

Table 4.1.2: Characteristics of the considered GNSS receivers.

Table 4.1.2 shows the main characteristics of the considered GNSS receivers. The information has been obtained from [51], [52], [53], [54] and [9].

According to what has been studied in Section 3.4, the accuracy provided by all the selected modules is enough for the mission. The most relevant aspect is the big discrepancy in power consumption, being around 100 mW for the GNSS200 and the piNAV-NG, while the NSS GPS and the OEM719 consume around 1 W.

Since the power, mass and volumetric payloads are tight in this mission, and they fulfill the requirements, the Hyperion GNSS200 and the SkyFoxLabs piNAV-NG are considered appropriate, while the rest are discarded. Moreover, since there is some missing information about the GNSS200, the piNAV-NG GNSS receiver has been chosen as the most suitable receiver for the OUFTI-Next satellite.

4.2 Communications

Next, the communications subsystem components are analysed. Having settled that the data download is performed using S-band, the components of the COMM system are the VHF/UHF transceiver, the S-band transmitter, and the antennas for both frequency bands.

4.2.1 Commands and telemetry

VHF/UHF transceiver

The commands uplink and the telemetry downlink communications are done by means of a VHF/UHF transceiver. Four of these units have been analysed: The EnduroSat UHF Transceiver Type II, the GOMSpace NanoCom AX100, the ISISpace TRXUV VHF/UHF Transceiver, and the NanoAvionics SatCOM UHF Digital Radio.

Table 4.2.1 shows the main characteristics of the considered transceiver units. The information has been extracted from [55], [56], [57] and [58].

Company	EnduroSat	GOMSpace	ISISpace	Nanoavionics
Name	UHF TRx II	AX100	TRXUV	SatCOM
Volume	0.11U	0.07U	0.15U	0.1U
Mass	94 g	24.5 g	85 g	60 g
Data rate	9600 bps	9600 bps	9600 bps	9600 bps
Power consumption	2 W (Tx) 85 mW (Rx)	2.6 W (Tx) 400 mW (Rx)	1.7 W (Tx) 200 mW (Rx)	2 W (Tx) -
Tx Power	33 dBm	30 dBm	23 dBm	33 dBm
Temperature	-35 to 80 °C	-30 to 85 °C	-10 to 45 °C	-40 to 85 °C
Heritage	Since 2018	Yes	Since 2016	Yes
Cost	\$4375	-	\$9500	-

Table 4.2.1: Characteristics of the considered VHF/UHF transceivers.

All of the selected transceivers provide similar values: Around 2 W in power consumption, 9600 bps in data rate, around 0.1U in volume and less than 100 g in weight. For this reason, in this case no specific unit is selected for being more fitting than the rest according to the mission requirements.

VHF/UHF antenna

Besides, an antenna needs to be selected to work with the VHF/UHF transceiver to perform the commands and telemetry communications. Most manufacturers provide antennas designed to work with their transceiver units. So, according to the previously displayed transceivers, the same company's antenna's characteristics are displayed in Table 4.2.2.

Company	EnduroSat	GOMSpace	ISISpace	Nanoavionics
Unit size	1U	2U	1U	1U
Mass	85 g	90 g	85 g	17 g
Gain	> 0 dBi	> -5 dBi	0 dBi	-
Power	10 mW	160 mW	40 mW	-
Temperature	-	-40 to 90 °C	-20 to 60 °C	-40 to 85 °C
Heritage	Since 2018	Yes	Since 2016	Yes
Cost	\$3750	-	\$5000	-

Table 4.2.2: Characteristics of the considered VHF/UHF antennas.

This information has been obtained from [59], [60], [61] and [58]. Once again, all units have similar characteristics. It is important to note that each antenna unit comes with its own active deployment system adapted for CubeSats. However, most of them are intended for 1U to 3U CubeSats.

The only one that presents a specific deployment system for 6U structures is the one by GOMSpace. For this reason, this antenna unit and the corresponding transceiver are selected as the reference VHF/UHF communications systems.

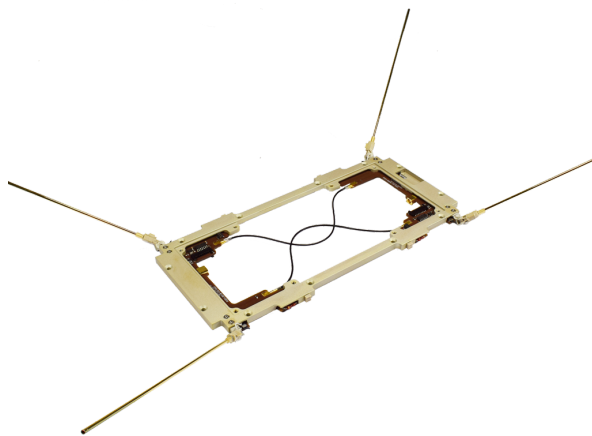


Figure 4.2.1: GOMSpace NanoCom ANT-6F antenna unit [60].

4.2.2 Data download

S-band transmitter

Moving on to data download, the needed transmitter operates in S-band in this case. Four different transmitters have been looked at, including the Clydespace CPUT S-band transmitter, the GOMspace NanoCom SR2000, IQ Wireless HiSPiCO and the ISISpace high data rate S-band transmitter. Their information can be found in [62], [63], [64], [65] and [57]; and is summarized in Table 4.2.3.

Company	Clydespace	GOMSpace	IQ Wireless	ISISpace
Name	CPUT S	SR2000	HiSPiCO	S-band Tx
Volume	0.2U	0.1U	0.15U	0.33U
Mass	100 g	271 g	100 g	300 g
Data rate	2 Mbps	2 Mbps	1.6 Mbps	3.4 Mbps
Power cons.	5 W	6 W	5 W	9.2 W
Tx Power	30 dBm	-	27 dBm	33 dBm
Temperature	-25 to 61 °C	-40 to 85 °C	-20 to 50 °C	-40 to 60 °C
Heritage	-	-	Since 2017	Since 2018
Cost	-	-	\$7300	-

Table 4.2.3: Characteristics of the considered S-band transmitters.

The units from Clydespace, GOMSpace and IQWireless provide roughly similar numbers, while the ISISpace transmitter is significantly bigger, provides a higher data rate and has a larger power consumption. Taking into account that the results obtained in Section 3.3 for 2 Mbps are more than enough, this unit is discarded.

Among the rest, the Clydespace CPUT transmitter has low power consumption and high transmitter power. However, no flight heritage has been found for this unit. Besides, the IQ Wireless HiSPiCO has plenty of flight heritage and has similar values for power and data rate, so this unit is selected as the most fitting for the OUFTI-Next demonstrator, keeping in mind that the Clydespace and GOMSpace options are also viable.

S-band antenna

Similarly to what has been explained for the VHF/UHF antennas, most of the available S-band antennas are linked to the transmitters, since the manufacturers usually design their antennas to work with their transmitter units.

For S-band, directional patch antennas are used, so their position on the satellite is relevant. The attitude for the communications operational mode must be to orient the antenna to the ground station, using the ADCS module. These antennas, however, do not require deployment mechanisms, so one less potential failure mode is present.

Table 4.2.4 displays the information about the considered patch antennas for S-band. This information has been obtained from [62], [65], [66] and [67].

Company	Clydespace	GOMSpace	IQ Wireless	EnduroSat
Size	1U	1U	1U	1U
Mass	50 g	110 g	75 g	64 g
Gain	7 dBi	8 dBi	6 dBi	8.3 dBi
Temperature	-40 to 85 °C	-45 to 85 °C	-40 to 65 °C	-
Heritage	-	-	Since 2017	-
Cost	-	-	\$5100	\$3000

Table 4.2.4: Characteristics of the considered S-band antennas.

Having determined that the HiSPiCO transmitter provides enough data rate and is the most fitting for the mission, the most suitable antenna for it is the one designed by IQ Wireless for this purpose. It presents similar characteristics to the rest of considered patch antennas.

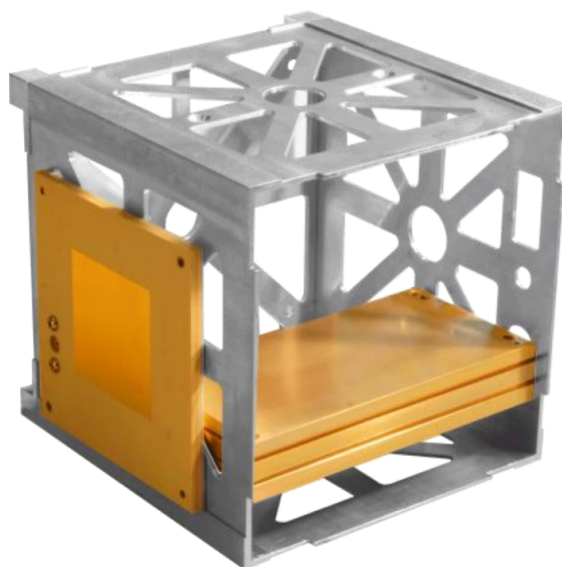


Figure 4.2.2: HiSPiCO S-band Tx and patch antenna mounted on a 1U [64].

4.3 Power

The next subsystem to be looked at is the electrical power system. This is composed of the EPS module including the battery packs, and the solar panels.

4.3.1 EPS module

In Section 3.5, several generic payloads have been analysed, obtaining values from 3 to 16 Wh for the minimum required battery capacity. This corresponds to what has been characterised as small (~ 10 Wh) and medium (~ 20 Wh) EPS integrated modules in Section 2.1.4.

Detailed information about these is presented in Table 4.3.1. The units present two values for volume, mass and battery capacity, since they admit two different battery packs. This information has been obtained from [68], [69], [70] and [24].

Company	Crystalspace	CubeSat Kit	EnduroSat	GOMSpace
Name	P1U Vasik	Linear EPS	EPS I / I Plus	P31u / P60
Volume	0.07 / 0.13 U	0.18 / 0.28 U	0.21 / 0.3 U	0.26 / 0.43 U
Mass	80 / 140 g	155 / 210 g	208 / 292 g	200 / 449 g
Power cons.	15 mW	100 mW	75 mW	160/600 mW
BP capacity	11 / 22 Wh	11 / 22 Wh	10.4 / 20.8 Wh	20 / 38.5 Wh
Max Power	10 W	15 W	20 W	30 / 60 W
Temperature	-40 to 85 °C	-40 to 85 °C	-40 to 150 °C	-40 to 85 °C
Heritage	Since 2013	-	Since 2018	Since 2013
Cost	\$4900	-	\$3125 / \$4125	-

Table 4.3.1: Characteristics of the considered EPS modules.

The main difference amongst similar-sized units is the maximum power output, which might not be enough for the power ranges envisaged in Section 3.5. So, only the EnduroSat and GOMSpace modules are considered fitting for the OUFTI-Next.

4.3.2 Solar panels

The required amount of solar panel units depends on each configuration. In any case, they are either grouped in a 6U surface for face X, a 3U surface for face Y, or a 2U surface for face Z on the satellite.

Different sizes of solar panels have been found, as well as solutions for deployable and non-deployable requirements. The selected units from EnduroSat, GOMSpace and ISISpace are described in Table 4.3.2, while the characteristics of units from Andrews Space and DHV Technology are displayed in Table 4.3.3. This information has been obtained from [71], [72], [73], [74], [75], [76], [77] and [78].

Company	EnduroSat	GOMSpace	ISISpace
Size	1U / 3U	1U / 3U	1U / 3U / 6U
Deployable	No / No	No / Yes	No / No / No
Mass	44 / 136 g	26 g / 150 g	50 / 150 g / 300 g
Number of cells	2 / 7	2 / 6	2 / 6 / 15
Cell area	60.30 / 211.05 cm ²	60.36 / 181.08 cm ²	-
Power	2.4 / 8.43 W	2.4 / 7.2 W	2.3 / 6.9 / 17.0 W
Temperature	-55 to 125 °C	-55 to 150 °C	-40 to 125 °C
Heritage	Since 2018	-	Since 2013
Cost	\$1700 / \$4800	-	\$2800 to \$5400

Table 4.3.2: Characteristics of the EnduroSat, GOMSpace & ISISpace solar panels.

Company	Andrews Space	DHV Technology
Size	6U	1U / 3U / 6U
Deployable	No	No / No / Yes
Mass	300 g	39 / 132 / 300 g
Number of cells	16	2 / 7 / 20
Power	19.4 W	2.4 / 8.48 / 20.0 W
Temperature	-25 to 150 °C	-120 to 150 °C
Heritage	-	Since 2014
Cost	\$17 500	-

Table 4.3.3: Characteristics of the Andrews Space & DHV Technology solar panels.

It is clear that fitting a higher number of cells in a 3U or a 6U unit can yield significantly greater values of power generation. For this reason, the units from DHV Technology have been selected as the most efficient.

Thus, the 6U and the 3U panel arrays from DHV are selected to go over the X face and the Y face of the satellite, respectively. This has the added advantage of being able to deploy the 6U arrays, if necessary.

Finally, the Z face of the satellite can be covered by two 1U units from any of the considered manufacturers, since they provide similar amounts of power generation from 2.3 to 2.4 W.

4.4 On-Board Computer

The selection of the OBC module needs to be done in later stages of the mission design, since the necessary memory and processing power depend on the selected payload and acquisition strategy, which are open questions for the moment.

Nevertheless, in the line of the present systems analysis, the main characteristics of some COTS OBC units are presented in Table 4.4.1, including ISISpace's iOBC, EnduroSat's OnBoard Computer, the NanoMind A3200 by GOMSpace and the CubeComputer v1.4 by CubeSpace. This information has been obtained from [79], [23], [80] and [81].

Company	ISISpace	EnduroSat	GOMSpace	CubeSpace
Name	iOBC	OBC	A3200	CubeComputer
Volume	0.12U	0.2U	0.07U	0.1U
Mass	76 g	58 g	24 g	56 g
Mean power	400 mW	340 mW	170 mW	200 mW
Peak power	550 mW	440 mW	900 mW	435 mW
Memory	64MB SDRAM, 1MB NOR Flash, 256kB FRAM, 2 MicroSD	2MB Program Memory, 256kB RAM, 2048kB flash, MicroSD socket	512KB flash, 128MB NOR flash, 32kB FRAM, 32MB SDRAM	23kB EEPROM, 4MB flash, 2MB SRAM, MicroSD socket
Processor	400MHz 32-bit	180 MHz 32-bit	64 MHz 32-bit	48 MHz 32-bit
Temperature	-25 to 65 °C	-30 to 85 °C	-30 to 85 °C	-10 to 70 °C
Heritage	Since 2014	Since 2018	Since 2015	Since 2018
Cost	\$4900	\$2900	\$7250	\$4500

Table 4.4.1: Characteristics of the considered OBC units.

4.5 Chassis

The last component in the systems analysis is the 6U structure for the satellite. Its job is to withstand the mechanical loads on the satellite, while holding all the subsystems in place.

In the same spirit as for the rest of subsystems, a COTS analysis has been performed so it can be used as reference in the future. The 6U structures provided by EnduroSat, GOMSpace and ISISpace have been considered. The mass, size and cost for each one is presented in Table 4.5.1, the information for which has been obtained from [82], [83] and [19].

Company	EnduroSat	GOMSpace	ISISpace
Mass	908 g	1060 g	698 g
Length	100 mm	100 mm	100 mm
Width	226.3 mm	226.3 mm	226.3 mm
Height	366 mm	340.5 mm	340.5 mm
Cost	\$8250	-	\$8300

Table 4.5.1: Characteristics of some COTS 6U structures.

It is important to keep in mind that the size of the structure needs to be selected in function of the size of the largest solar panels that need to be attached to it. For a 6U CubeSat, these can be up to $100.0 \times 226.3 \times 366.0$ according to the design specifications [20].

Having selected the 6U DHV technologies solar arrays, the best option is the 6U structure by Endurosat, as it secures enough room for the solar panels. In later stages of the satellite's design, this choice needs to be revisited taking into account the structural requirements.

Chapter 5

Proposed configurations

After selecting the most fitting units for the satellite in each subsystem, some full satellite configurations are proposed for the 6U OUFTI-Next satellite. Since the payload for this is still an open discussion, three proposals are made in this chapter, for three payload sizes.

These configurations have been named OUFTI-Next 6S, 6M and 6L. This way, once the mission's payload systems are fully settled, the most fitting solution amongst these proposals can be taken.

5.1 OUFTI-Next 6S

The first proposed arrangement aims to efficiently carry payloads with low requirements in power. In Section 3.5, the preliminary configuration 1 has turned out to be feasible for scenarios where the payload power requirements are low, and so, communications are limiting.

With this in mind, the OUFTI-Next 6S has the external shape of configuration 1, with 6U of solar panels mounted on the satellite's X face, and it is sized so it can perform communications with the ground station at every available pass, as well as performing reliable data acquisition.

For this, the EnduroSat EPS Type I has been selected, providing 11 Wh in battery capacity and a maximum power capacity of 20W, which matches the power generated by the solar cells.

5.1.1 Components

The components of the OUFTI-Next 6S platform are fully defined. In Table 5.1.1, these units are displayed with their mass, dimensions, volume allocated in the structure, and cost.

Component	Mass	Dimensions (Allocated volume)	Cost
ADCS Module BlueCanyon XACT-50	1230 g	100×100×75.4 mm (0.75U)	\$125 000
GNSS Receiver SkyFoxLabs piNAV-NG	24 g	71.1×45.7×11 mm (0.15U)	\$6900
VHF/UHF Transceiver GS NanoCom AX100	25 g	65×40×6.5 mm (0.15U)	-
VHF/UHF Antenna GS NanoCom ANT-6F	90 g	116.7×221.7×9.1 mm (+Z face frame)	-
S-band Tx IQ Wireless HiSPiCO	100 g	95×46×15 mm (0.20U)	\$7300
S-band Antenna IQ Wireless HiSPiCO	75 g	50×50×3.2 mm (TBD)	\$5100
OBC EnduroSat OBC	58 g	95.9×90.2×23.2 mm (0.25U)	\$2900
EPS Module EnduroSat EPS Type I	208 g	95.9×90.2×21.2 mm (0.22U)	\$3125
Solar Array DHV 6U Fixed Panels	300 g	360×189.5×1.6 mm (+X face frame)	-
Structure EnduroSat 6U Structure	908 g	366×226.3×100 mm	\$8250
Platform Total	3018 g	(1.00U + ADCS) 1.75 U	\$158 575 ¹

Table 5.1.1: Mass, volume and cost budget for the OUFTI-Next 6S platform.

The obtained total mass of the platform is slightly above 3 kg. For the volume, all subsystems except for the ADCS module fit into a 1U space, taking plenty of breathing space between PCBs. The ADCS itself occupies 0.75U, so a total of 1.75U is required for the platform in the OUFTI-Next 6S.

¹Incomplete value: Information about the cost of the VHF/UHF COMM system and solar panels is missing. With values for similar products, the total cost is estimated around \$175 000.

This means that, regarding the mechanical aspects, this configuration allows for any payload of less than 8.9 kg in weight and 4.25U in total size. The limitations in power consumption are discussed in the next section.

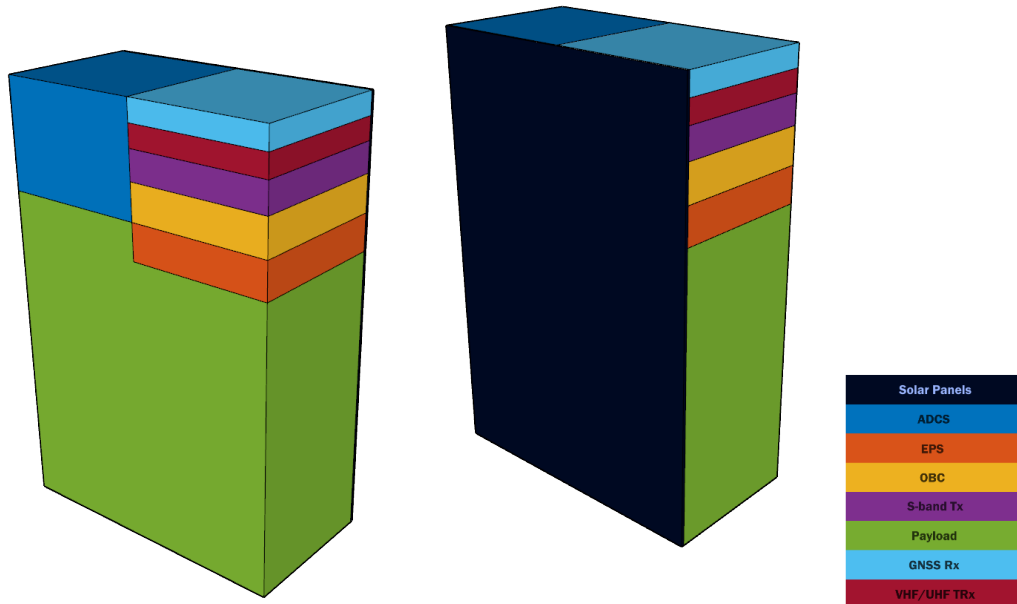


Figure 5.1.1: Arrangement of the OUFTI-Next 6S. Front and back.

5.1.2 Power budget

The power consumption of each of the selected components is shown in Table 5.1.2 for each of the operational modes defined in the mission analysis.

	Mode 1	Mode 2	Mode 3	Mode 4
ADCS Module	2470 mW	2470 mW	2470 mW	500 mW
GNSS Rx	125 mW	125 mW	125 mW	125 mW
VHF/UHF TRx	0 mW	2600 mW	0 mW	0 mW
VHF/UHF Antenna	0 mW	160 mW	0 mW	0 mW
S-band Tx	0 mW	5000 mW	0 mW	0 mW
S-band Antenna	0 mW	500 mW	0 mW	0 mW
OBC	440 mW	440 mW	440 mW	440 mW
EPS	75 mW	75 mW	75 mW	75 mW
Platform Total	3110 mW	11 370 mW	3110 mW	1140 mW

Table 5.1.2: 6S Configuration power consumption for each operational mode.

The used operational modes are: Sun-pointing power generation (Mode 1), communications with the ground station (Mode 2), Earth observation (Mode 3), and idle mode during eclipse (Mode 4).

Using the simulations performed in Section 3.5 and the selected solar panels, the average power generated in sun-pointing and nadir-pointing attitude is presented in Table 5.1.3.

Sun pointing	Nadir pointing
20.00 W	12.75 W

Table 5.1.3: 6S Configuration average generated power for Sun and nadir pointing.

With this, the performance of the OUFTI-Next 6S configuration is assessed in the operational scenarios proposed in Section 3.5, these being an orbit without events (Scenario 1), an orbit with a COMM pass during illumination (Scenario 2), an orbit with a COMM pass during eclipse (Scenario 3) and an orbit including a 10-minute Earth observation pass during illumination (Scenario 4).

In this case, the communications pass is the limiting factor for the achievable idle mode payload power consumption, which is up to 5.56 W. For this maximum value, the maximum power output of the EPS module sets the maximum payload power consumption in operation. For clarity, these are displayed in Table 5.1.4.

Operational mode	Idle mode
16.89 W	5.56 W

Table 5.1.4: 6S Configuration maximum payload power consumption.

5.2 OUFTI-Next 6M

The second proposed configuration has the objective of fulfilling the missions for which the OUFTI-Next 6S is insufficient in terms of power.

Taking into account the general results obtained in Chapter 3, configuration 2 has been selected. This setup, including non-deployable solar panels in all three faces of the satellite, allows to increase the power production especially when performing nadir-pointing maneuvers. Not having deployable panels also has the advantage of entirely avoiding this potential failure point, which can eventually compromise other subsystems.

5.2.1 Components

This arrangement includes the same selected systems as the previous one, upgrading the EPS module to the GOMSpace P31u and including the additional fixed solar panels. The new EPS allows for power values up to 30 W and includes a total battery capacity of 20 Wh.

Component	Mass	Dimensions (Allocated volume)	Cost
ADCS Module BlueCanyon XACT-50	1230 g	100×100×75.4 mm (0.75U)	\$125 000
GNSS Receiver SkyFoxLabs piNAV-NG	24 g	71.1×45.7×11 mm (0.15U)	\$6900
VHF/UHF Transceiver GS NanoCom AX100	25 g	65×40×6.5 mm (0.15U)	-
VHF/UHF Antenna GS NanoCom ANT-6F	90 g	116.7×221.7×9.1 mm (+Z face frame)	-
S-band Tx IQ Wireless HiSPiCO	100 g	95×46×15 mm (0.20U)	\$7300
S-band Antenna IQ Wireless HiSPiCO	75 g	50×50×3.2 mm (TBD)	\$5100
OBC EnduroSat OBC	58 g	95.9×90.2×23.2 mm (0.25U)	\$2900
EPS Module GS NanoPower P31u	200 g	92.9×89.3×24.2 mm (0.25U)	-
Solar Array DHV 6U Fixed Panels	300 g	360×189.5×1.6 mm (+X face frame)	-
Solar Array DHV 3U Fixed Panels	132 g	329×82×1.6 mm (+Y face frame)	-
Solar Array 2 DHV 1U Fixed Panels	78 g	97×97×1.6 mm (+Z face frame)	-
Structure EnduroSat 6U Structure	908 g	366×226.3×100 mm	\$8250
Platform Total	3480 g	(1.00U + ADCS) 1.75 U	\$155 450 ²

Table 5.2.1: Mass, volume and cost budget for the OUFTI-Next 6M platform.

²Incomplete value: The cost of the VHF/UHF COMM system, EPS module and solar panels is missing. With values for similar products, the total cost is estimated around \$180 000.

Table 5.2.1 includes the mass, dimensions, volume allocated in the structure, and cost of all components of the 6M configuration.

These can fit in the structure in same way as the 6S, with all the components except for the 0.75U ADCS module included in a 1U cube. So, the available volume for the payload systems is 4.25U once again. The weight, however, has increased with the EPS upgrade, coming to a total of 3220 g. This means that the payload systems can have a maximum mass of up to around 8.5 kg.

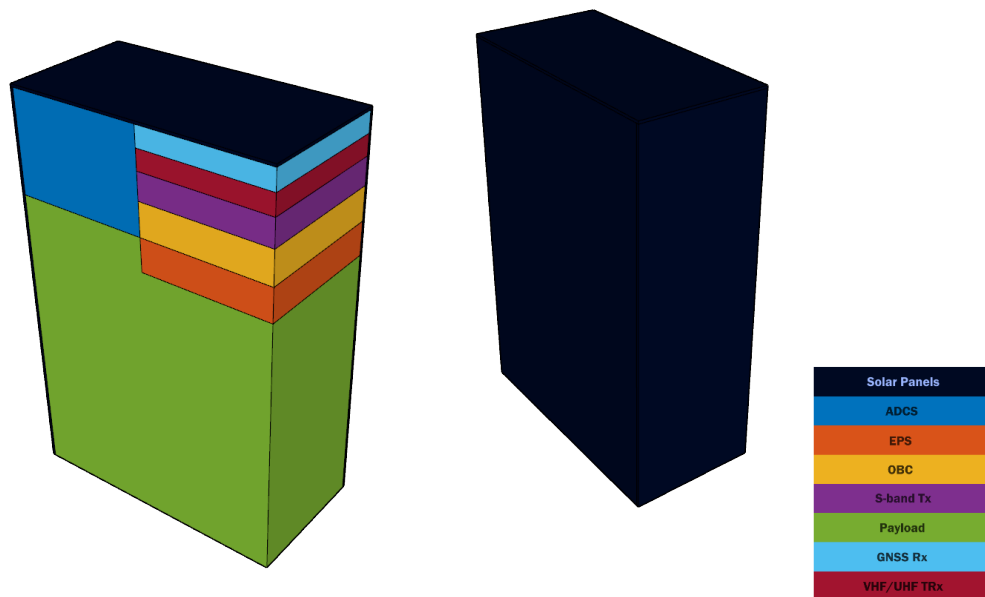


Figure 5.2.1: Arrangement of the OUFTI-Next 6M. Front and back.

5.2.2 Power budget

With the upgrade in EPS, the power consumption of this unit is increased to 160 mW. This affects the total power consumption values in all of the mission's operational modes. Since most of the values have already been presented in Table 5.1.2, only the total power consumption in each mode is presented in Table 5.2.2, so no redundant information is shown.

	Mode 1	Mode 2	Mode 3	Mode 4
Platform Total	3195 mW	11 455 mW	3195 mW	1125 mW

Table 5.2.2: 6M Configuration power consumption for each operational mode.

The generated power is different too, since the solar arrays have been upgraded. Once again, the performed simulations yield the average power generation values shown in Table 5.2.3.

Sun pointing	Nadir pointing
22.25 W	14.18 W

Table 5.2.3: 6M Configuration average generated power for Sun and nadir pointing.

In this case, the most efficient Sun pointing attitude is a rotation of 23.0° around the Z axis, plus a rotation of 12.5° around the resulting Y' axis, in the satellite reference frame. Once again, the nadir-pointing attitude result is used for estimating the power generation during modes 2 and 3.

With this, the proposed operational scenarios are used to size the allowable payload power consumption in operative and idle mode, knowing that the battery capacity is 20 Wh and the total power cannot exceed 30 W.

In this case, the acquisition scenario is the one that limits the maximum idle power consumption of the payload, when imposing that the battery depth of discharge must be above 50% and that it needs to be able to recharge back to 100% after each orbit.

Besides, the maximum power consumption attainable by the payload in operational mode is limited by the Electrical Power System's capabilities. These values are displayed in Table 5.2.4.

Operational mode	Idle mode
26.80 W	10.14 W

Table 5.2.4: 6M Configuration maximum payload power consumption.

This upgrade allows to boost the power of the payload by around 10 W, also allowing twice the previously available idle power consumption. However, both maximum values aren't attainable at the same time, as in that case, the power generation isn't sufficient.

This situation arises for a small range of values near the maximum in idle and operational power consumption, which are characterised in Section 5.4.

5.3 OUFTI-Next 6L

The third and final proposed configuration is intended for payloads with high values of power consumption. Section 3.5 has identified the preliminary configuration 4 as more efficient than the similar configurations with two deployed solar panels, while the more complex solutions with three or four deployed solar arrays have resulted unnecessary.

For this reason, the OUFTI-Next 6L configuration takes the concept of the preliminary configuration 4, with a fix 2U solar array on the +Z face, plus two 6U deployable solar panels from faces +X and -X. Thus, creating a large solar array surface on the +Z face of the satellite.

It is important to keep in mind that solar panel deployment adds a failure mode to the mission, since un-deployed solar panels can potentially impair the operation of other subsystems.

5.3.1 Components

This arrangement includes the same general components as the two previously presented configuration, once again upgrading the electrical power system and the solar panels.

In the OUFTI-Next 6L configuration, the selected electrical power system is the GOMSpace NanoPower P60, which allows for a maximum power of 60 W across the system. Besides, the selected battery pack to go with it is the GOMSpace NanoPower BP4, which is designed to work with the selected EPS and provides a total of 38.5 Wh in battery capacity.

Regarding the distribution, the GNSS receiver, VHF/UHF transceiver, S-band transmitter, OBC and EPS modules can fit once again in a 1U cube. Besides, the 0.25U allocated for the batteries is placed over the ADCS module, bringing the total volume required by the platform to 2U. The mass of the upgraded platform becomes 3635 g, so all the payload systems can amount up to 8.3 kg in mass and 4U in volume. This is slightly less than the smaller configurations, still staying in the same order of magnitude.

Finally, like in the previous configurations, the mass, dimensions, volume allocated in the structure and cost of all the components present in the 6L configuration are shown in Table 5.3.1.

Component	Mass	Dimensions (Allocated volume)	Cost
ADCS Module BlueCanyon XACT-50	1230 g	100×100×75.4 mm (0.75U)	\$125 000
GNSS Receiver SkyFoxLabs piNAV-NG	24 g	71.1×45.7×11 mm (0.15U)	\$6900
VHF/UHF Transceiver GS NanoCom AX100	25 g	65×40×6.5 mm (0.15U)	-
VHF/UHF Antenna GS NanoCom ANT-6F	90 g	116.7×221.7×9.1 mm (+Z face frame)	-
S-band Tx IQ Wireless HiSPiCO	100 g	95×46×15 mm (0.20U)	\$7300
S-band Antenna IQ Wireless HiSPiCO	75 g	50×50×3.2 mm (TBD)	\$5100
OBC EnduroSat OBC	58 g	95.9×90.2×23.2 mm (0.25U)	\$2900
EPS Module GOMSpace NanoPower P60	179 g	92×88.9×19.8 mm (0.25U)	-
Battery pack GOMSpace NanoPower BP4	270 g	94×84×23 mm (0.25U)	-
Solar Array 2 DHV 6U Deployable Panels	600 g	360×189.5×1.6 mm (±X face frames)	-
Solar Array 2 DHV 1U Fixed Panels	78 g	97×97×1.6 mm (+Z face frame)	-
Structure EnduroSat 6U Structure	908 g	366×226.3×100 mm	\$8250
Platform Total	3637 g	2.00 U	\$155 450 ³

Table 5.3.1: Mass, volume and cost budget for the OUFTI-Next 6L platform.

5.3.2 Power budget

The power consumption of all subsystems except for the EPS is the same as for the OUFTI-Next 6S and 6M. In this case, the selected EPS has a consumption of 600 mW. Including this, and once again avoiding the information already displayed in Table 5.1.2, the power consumption for each operational mode of the OUFTI-Next 6L is shown in Table 5.3.2.

³Incomplete value: The cost of the VHF/UHF COMM system, EPS system and solar panels is missing. With values for similar products, the total cost is estimated around \$190 000.

	Mode 1	Mode 2	Mode 3	Mode 4
Platform Total	3635 mW	11 895 mW	3635 mW	1665 mW

Table 5.3.2: 6L Configuration power consumption for each operational mode.

Besides, the power generation in this case is significantly increased, especially in nadir-pointing, due to the deployed solar panel configuration. The results of the simulations with the selected panels are shown in Table 5.3.3.

Sun pointing	Nadir pointing
44.80 W	43.46 W

Table 5.3.3: 6L Configuration average generated power for Sun and nadir pointing.

Finally, the same operational scenario study is performed in order to determine the maximum power consumption of the payload in this configuration. Similarly to the 6M, the acquisition scenario sets the limit for the idle power consumption of the payload, while the maximum for operation is defined by the EPS capacity. The results for maximum payload power consumption are displayed in Table 5.3.4.

Operational mode	Idle mode
56.36 W	22.34 W

Table 5.3.4: 6L Configuration maximum payload power consumption.

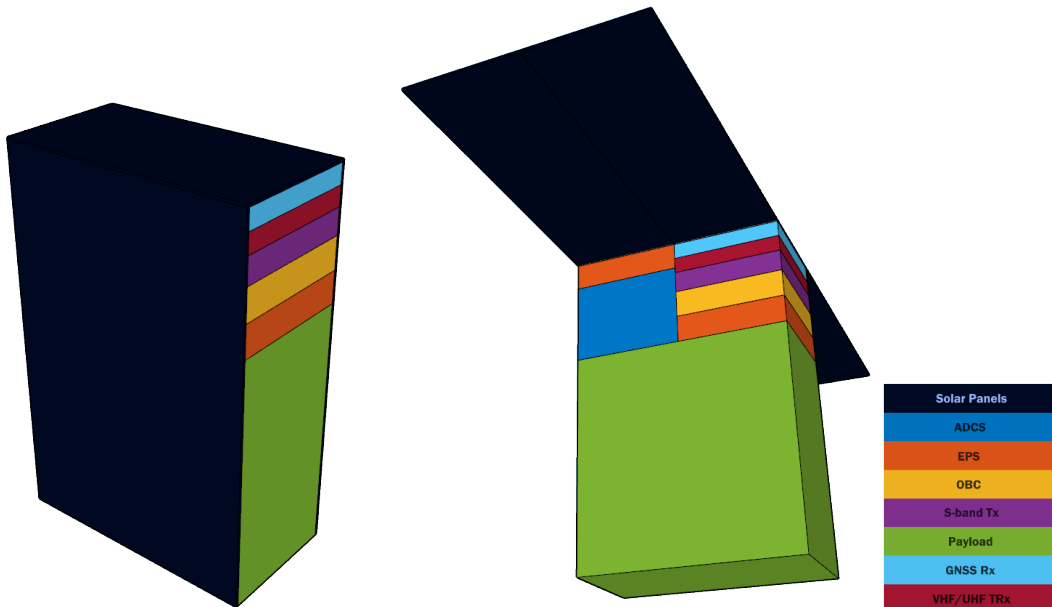


Figure 5.3.1: Arrangement of the OUFTI-Next 6L. Packed and deployed.

5.4 Summary

Next, the three proposed configurations are presented side by side, so a global view of which one to choose, given a payload, is provided. Tables 5.4.1 and 5.4.2 display the values for mass, volume and estimated cost of the platform, as well as the maximum attainable payload mass, volume and power in idle and operational mode.

	OUFTI-Next 6S	OUFTI-Next 6M	OUFTI-Next 6L
Mass	3.02 kg	3.48 kg	3.64 kg
Volume	1.75 U	1.75 U	2.00 U
Estimated cost	\$175 000	\$180 000	\$190 000

Table 5.4.1: Platform features of the OUFTI-Next 6S, 6M and 6L.

	OUFTI-Next 6S	OUFTI-Next 6M	OUFTI-Next 6L
Mass	8.9 kg	8.5 kg	8.3 kg
Volume	4.25 U	4.25 U	4.00 U
Max. idle power	5.56 W	10.14 W	22.34 W
Max. power	16.89 W	26.80 W	56.36 W

Table 5.4.2: Maximum payload features of the OUFTI-Next 6S, 6M and 6L.

Finally, Figure 5.4.1 graphically displays all the feasible values of idle and operational power consumption of the payload, by the three configurations. In later stages in the mission's development, this information can be used to easily determine the most fitting configuration of the 6U OUFTI-Next CubeSat.

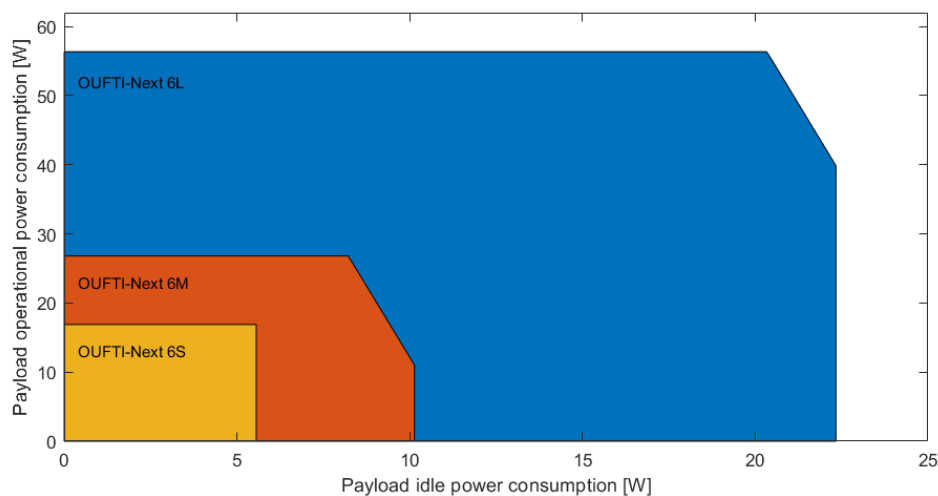


Figure 5.4.1: Payload power consumption of the OUFTI-Next 6S, 6M and 6L.

Chapter 6

Conclusions

This study needs to be understood in the context of the larger OUFTI-Next project. The need for this analysis comes out of the proposal for an upgraded payload in the satellite, which requires an upgraded platform.

With the currently still open discussion about the payload, the main idea that has been pursued is to propose a set of working satellite platforms that can adapt to a wide range of potential payloads, as well as to define concise orders of magnitude for any 6U solution for the OUFTI-Next demonstrator.

The first step in this direction has been taken in the proposal of eight preliminary panel arrangements. These have provided insightful reference values for the systems on the satellite, and they have also confirmed that, in the case of a failure in the deployment of solar panels, the reduced array arrangements can be enough to power the platform.

Next, a more detailed analysis of the main aspects of the mission has been carried out, setting a viable altitude range for the final mission regarding launch opportunities and orbit lifetime. Besides, the selection of a frequency band for data download has been settled with S-band, since VHF is not enough for reliable data download, and X-band is an unnecessarily powerful technology.

The following commercial units research and analysis has provided a selection of the ideal components for each subsystem, as well as characterising the rest as acceptable or unfeasible. The most fitting of these have been included in the proposed platform configurations.

Concerning the total costs of each proposed configuration, the largest part is related to the selected Blue Canyon XACT-50 ADCS integrated module. In spite of its high cost, it is the only considered one with available proof of fulfilling the

set requirements for pointing accuracy and stability in previous missions. However, this choice has little impact on the mass, volumetric and power budget of the final configurations, as it can be easily exchanged by any other ADCS module that can fulfill the requirements.

Should this be done, and an ADCS module with higher power consumption be selected, this difference can be deducted from the payload's total idle power consumption, making the developed power budget analysis still applicable. So, keeping this in mind, the choices in almost all components are easily interchangeable with little to no effect on the general performance of the three proposed platforms. The only key units are the ones directly linked to the power and communications systems.

This study has therefore given three working proposals for 6U configurations of the OUFTI-Next demonstrator, each one specifically designed for a range in payload power consumption. In regard to the mass and volume, the conclusion is that payloads of under 9 kg in mass and volumes of 4U or slightly more are supported in this CubeSat dimensions.

The next steps to be taken in the development of the 6U configuration OUFTI-Next satellite require definite information about the payload systems. Once this is settled, a detailed thermal analysis needs to be performed, as well as an assessment of the Attitude Determination and Control System.

Bibliography

- [1] Dimitry Schklar, *OUFTI-Next Nanosatellite: Feasibility Study and Mission Assessment*. University of Liège, 2016-2017. Master's thesis.
- [2] Enrico Ghidoli, *Feasibility Study of a Mid-wave Infrared CubeSat for Smart Irrigation of Agricultural Fields - "OUFTI-NEXT"*. University of Liège, 2016-2017. Master's thesis.
- [3] Colin Dandumont, *From mission analysis to systems engineering of the OUFTI-Next nanosatellite*. University of Liège, 2017-2018. Master's thesis.
- [4] Pierre Remacle, *Study of a cooling system for a CubeSat infrared detector*. University of Liège, 2017-2018. Master's thesis.
- [5] Anna Riera Salvà, *OUFTI-Next: Design of refractive lenses for an infrared camera*. University of Liège, 2017-2018. Master's thesis.
- [6] Donatien Calozet, *Study of a IR reflective optical system for Earth observation from a 3U CubeSat*. University of Liège, 2017-2018. Master's thesis.
- [7] Lidiia Suleimanova, *Compact thermal IR imager based on flat Fresnel double lens for Smart Irrigation of Agricultural Fields - "OUFTI-NEXT"*. University of Liège, 2017-2018. Master's thesis.
- [8] Anthony Kellens, *Thermal design of the OUFTI-Next mission*. University of Liège, 2017-2018. Master's thesis.
- [9] Cristiano Contini, *OUFTI-Next ADC subsystem*. University of Liège, 2017-2018. Master's thesis.
- [10] Victor Laborde, *Study and development of innovative optical systems for infrared remote sensing on board nano satellite*. University of Liège. PhD.
- [11] Jesús Vilaboa Pérez, *Multi-band IR sensor for Earth observation*. University of Liège, 2018-2019. Master's thesis.
- [12] Antonio Dueñas Herrero, *Study of a CubeSat dual band infrared imager for hydric stress observation from space*. University of Liège, 2018-2019. Master's thesis.

-
- [13] Ysaline Bertrand, *Space validation of infrared materials for multispectral imager onboard a CubeSat mission*. University of Liège, 2018-2019. Master's thesis.
- [14] Bao Long Le Van, *Integrated thermal design of OUFTE-Next*. University of Liège, 2018-2019. Master's thesis.
- [15] Yuriko Osakabe, Keishi Osakabe, Kazuo Shinozaki, and Lam-Son P. Tran, "Response of plants to water stress," *Front Plant Sci.*, pp. 5–86, 03 2014.
- [16] C. J. Howarth, "Molecular responses of plants to an increased incidence of heat shock," *Plant, Cell & Environment*, pp. 831–841, 10 1991.
- [17] Nibir K. Dhar, Ravi Dat and Ashok K. Sood, "Advances in Infrared Detector Array Technology," *Optoelectronics - Advanced Materials and Devices*, 1 2013.
- [18] Planetary Resources, "Arkyd-6 Mission." <https://www.planetaryresources.com/missions/arkyd-6/>. Accessed 26/05/2019.
- [19] ISISpace, "6-Unit CubeSat structure." <https://www.isispace.nl/product/6-unit-cubesat-structure>. Accessed 25/05/2019.
- [20] The CubeSat Program, *6U CubeSat Design Specification*. California Polytechnic State University, 2018.
- [21] KU Leuven, *KU Leuven ADCS*. <http://www.cubesatpointing.com/DownloadFiles/Datasheets/KULADCSDatasheet.pdf>. Accessed 18/03/2019.
- [22] EnduroSat, *X-band Transmitter*. https://cdn5.endurosat.com/modules-datasheets/X_Band_Datasheet_Rev_1.1.pdf. Accessed 16/03/2019.
- [23] ISISpace, *iOBC On Board Computer*. <https://www.isispace.nl/wp-content/uploads/2016/02/iOBC-Brochure-v1.pdf>. Accessed 26/03/2019.
- [24] GOMSpace, *NanoPower P31u*. <https://gomspace.com/UserFiles/Subsystems/datasheet/gs-ds-nanopower-p31u-27.pdf>. Accessed 18/03/2019.
- [25] CNES, *STELA User Guide v3.2*, 2017. Available at: <https://logiciels.cnes.fr/fr/node/36?type=doc>.
- [26] ISISpace, "Launch Services." <https://www.isispace.nl/launch-services/>. Accessed 06/03/2019.
- [27] Spaceflight, "Launch Services." <http://spaceflight.com/schedule-pricing>. Accessed 06/03/2019.
- [28] RocketLab, "Launch Services." <https://www.rocketlabusa.com/book-my-launch>. Accessed 06/03/2019.

-
- [29] JAXA, “J-SSOD.” <https://www.jamss.co.jp/en/business/deployment.html>. Accessed 06/03/2019.
- [30] Robert T. Adams, *NanoRacks DoubleWide Deployer System Interface Definition Document*. NanoRacks, 2017.
- [31] bSpace, “Launch Services.” <http://www.bspacelaunch.com>. Accessed 07/03/2019.
- [32] Inter-Agency Space Debris Coordination Committee, *IADC Space Debris Mitigation Guidelines*, 2007.
- [33] Bruce R. Bowman, W Kent Tobiska, Frank A. Marcos and Cesar Valladares, “The JB2006 empirical thermospheric density model,” *Journal of Atmospheric and Solar-Terrestrial Physics*, vol. 70, pp. 774–793, 03 2008.
- [34] Tiera Laitinen, Juho Iipponen, Ilja Honkonen, Max van de Kamp, Ari Viljanen and Pekka Janhunen, *Thermospheric density variations due to space weather*. Finnish Meteorological Institute, ESA Earth, 2014.
- [35] Li Qiao, Chris Rizos and Andrew G. Dempster, *Analysis and Comparison of CubeSat Lifetime*. Australian Centre for Space Engineering Research, University of New South Wales, Sydney, Australia, 2012.
- [36] Heavens Above, “ISS Orbit.” <https://www.heavens-above.com/orbit.aspx?satid=25544>. Accessed 25/05/2019.
- [37] Masahiko Yamazaki, *Communication & Ground Station*. Department of Aerospace Engineering, College of Science and Technology, Nihon University, Japan. [http://www.unisec.jp/cltp/online/7\)CLTP4_Communication%20%20GroundStation.pdf](http://www.unisec.jp/cltp/online/7)CLTP4_Communication%20%20GroundStation.pdf). Accessed 21/04/2019.
- [38] FLIR, *Hot FPA technology for Swap+C optimized MWIR camera core*. <https://www.flir.com/globalassets/imported-assets/document/neutrino-lc-datasheet.pdf>. Accessed 04/05/2019.
- [39] Semi Conductor Devices USA, *Bird XGA*. <https://scdusa-ir.com/wp-content/uploads/2017/09/BIRD-XGA-1024x768-17um-pixel-pitch-V0x-Microbolometer.pdf>. Accessed 04/05/2019.
- [40] GOMSpace, *NanoCam C1U*. <https://gomspace.com/UserFiles/Subsystems/datasheet/gs-ds-nanocam-c1u-17.pdf>. Accessed 04/05/2019.
- [41] George Sebestyen, Steve Fujikawa, Nicholas Galassi and Alex Chuchra, *Low Earth Orbit Satellite Design*. Springer, 2018.

-
- [42] CNES, *Simu-CIC User Manual*, 2018.
- [43] Blue Canyon Technologies, *XACT-50 ADCS*. https://storage.googleapis.com/blue-canyon-tech-news/1/2019/05/BCT_DataSheet_Components_ACS.pdf. Accessed 18/03/2019.
- [44] Erik Kerstel, Arnaud Gardelein, Mathieu Barthelemy, CSUG, Matthias Fink, Siddarth Koduru Joshi and Rupert Ursin, “Nanobob: A Cubesat Mission Concept For Quantum Communication Experiments In An Uplink Configuration,” *EPJ Quantum Technology*, vol. 5, p. 6, Jun 2018.
- [45] NASA, *Small Spacecraft Technology State of the Art*. Ames Research Center, 2015. https://www.nasa.gov/sites/default/files/atoms/files/small_spacecraft_technology_state_of_the_art_2015_tagged.pdf. Accessed 09/03/2019.
- [46] Cube Space, *CubeADCS 3-axis*. https://www.cubesatshop.com/wp-content/uploads/2016/06/CubeADCS_3Axis_Specsheet_V1.0.jpg. Accessed 18/03/2019.
- [47] CubeSpace, *CubeADCS: The complete ADCS solution*, 2017. <https://cubespace.co.za/ClientDownloads/CubeADCS%20-%20ICD%20%5BV3.04%5D.pdf>. Accessed 01/04/2019.
- [48] Emanuela Della Bosca, *The DUST Tech Demo: an Intersatellite Communications Mission*. University of Michigan, 2017. <http://mstl.atl.calpoly.edu/~bklofas/Presentations/SummerWorkshop2017/Mckague.pdf>. Accessed 01/04/2019.
- [49] Hyperion Technologies B.V., *Hyperion-iADCS400*. https://hyperiontechnologies.nl/wp-content/uploads/2018/07/HT-iADCS400-V1.02_Flyer.pdf. Accessed 18/03/2019.
- [50] Kleine Ruimtevaart, *Hyperion Technologies Kivi Symposium*. Hyperion Technologies, 2017. <https://www.kivi.nl/uploads/media/58b03b4385a8f/Ruimtevaart-Bert%20Monna-Hyperion.pdf>. Accessed 01/04/2019.
- [51] Hyperion Technologies, *GNSS200 Series Global Navigation Receiver*, 2018. https://hyperiontechnologies.nl/wp-content/uploads/2018/07/HT-GNSS200-V1.3_Flyer.pdf. Accessed 14/05/2019.
- [52] SkyFoxLabs, *piNAV-NG GNSS Receiver*, 2018. http://www.skyfoxlabs.com/pdf/piNAV-NG_Datasheet_rev_F.pdf. Accessed 14/05/2019.

-
- [53] NewSpace Technologies, *GNSS200 Series Global Navigation Receiver*, 2018. https://www.cubesatshop.com/wp-content/uploads/2016/07/NewSpace-GPS-Receiver_8b.pdf. Accessed 14/05/2019.
- [54] NovAtel, *OEM719 Receiver*, 2018. <http://www.pumpkininc.com/space/datasheet/OEM719-Product-Sheet.pdf>. Accessed 14/05/2019.
- [55] EnduroSat, *UHF Transceiver Type II*. https://cdn4.endurosat.com/modules-datasheets/UHF_type_II_User_Manual_Rev_1.5.pdf. Accessed 16/03/2019.
- [56] GOMSpace, *NanoCom AX100*. <https://gomspace.com/UserFiles/Subsystems/datasheet/gs-ds-nanocom-ax100-33.pdf>. Accessed 16/03/2019.
- [57] ISISpace, *Communication Systems Brochure*. <https://www.isispace.nl/wp-content/uploads/2016/02/ISIS-Communication-systems-Brochure-v2-compressed.pdf>. Accessed 16/03/2019.
- [58] NanoAvionics, “Flight proven subsystems.” <https://n-avionics.com/subsystems/>. Accessed 16/03/2019.
- [59] EnduroSat, *UHF Antenna II*, 2018. https://cdn4.endurosat.com/modules-datasheets/UHF_Antenna_II_User_Manual_Rev1.4.pdf. Accessed 21/05/2019.
- [60] GOMSpace, *NanoCom Ant-6f UHF*, 2018. <https://gomspace.com/UserFiles/Subsystems/datasheet/gs-ds-nanocom-ant6f-uhf-20.pdf>. Accessed 21/05/2019.
- [61] ISISpace, *Antenna Systems*, 2017. <https://www.isispace.nl/wp-content/uploads/2016/02/ISIS-Antenna-systems-Brochure-v1.pdf>. Accessed 21/05/2019.
- [62] Clydespace, *CPUT S-Band transmitter*. <http://www.cput.ac.za/blogs/f sati/files/2016/07/BR-01-00017-STX-Brochure-Rev-B-Website.pdf>. Accessed 16/03/2019.
- [63] GOMSpace, *NanoCom SR2000*. <https://gomspace.com/UserFiles/Subsystems/datasheet/gs-ds-nanocom-sr2000-20.pdf>. Accessed 16/03/2019.
- [64] IQ Wireless, *HiSPiCO*. https://www.iq-spacecom.com/images/downloads/HiSPiCO_datasheet.pdf. Accessed 16/03/2019.
- [65] IQ Wireless, *Highly Integrated S Band Transmitter for Pico and Nano Satellites*. http://www.iq-wireless.com/images/pdf/HiSPiCO_Datasheet-en.pdf. Accessed 21/05/2019.

-
- [66] GOMSpace, *NanoCom ANT2000*. <https://gomspace.com/UserFiles/Subsystems/datasheet/gs-ds-nanocom-ant2000-11.pdf>. Accessed 21/05/2019.
- [67] EnduroSat, *S-Band Patch Antenna Type I*, 2018. https://cdn4.endurosat.com/modules-datasheets/S-Band_Patch_User_Manual_Rev1_2.pdf. Accessed 21/05/2019.
- [68] Crystalspace, *P1U Vasik Power Supply*. <http://crystalspace.eu/wp-content/uploads/2014/05/P1U-Power-Supply-summary-v1.pdf>. Accessed 18/03/2019.
- [69] CubeSat Kit, *Linear EPS*. http://www.cubesatkit.com/docs/datasheet/DS_CSK_Linear_EPS_711-00338-D.pdf. Accessed 18/03/2019.
- [70] EnduroSat, *Electrical Power System (EPS I & EPS I Plus)*. https://cdn5.endurosat.com/modules-datasheets/EPS_User_Manual_Rev_2.pdf. Accessed 18/03/2019.
- [71] EnduroSat, *1U Solar Panel*. https://cdn5.endurosat.com/modules-datasheets/Solar-Panel_1U_User_Manual_Rev1_5.pdf. Accessed 12/05/2019.
- [72] EnduroSat, *3U Solar Panel*. https://cdn5.endurosat.com/modules-datasheets/Solar-Panel_3U_User_Manual_Rev1.3.pdf. Accessed 12/05/2019.
- [73] GOMSpace, *NanoPower P110*. <https://gomspace.com/UserFiles/Subsystems/datasheet/gs-ds-nanopower-p110-210.pdf>. Accessed 12/05/2019.
- [74] GOMSpace, *NanoPower DSP*. <https://gomspace.com/UserFiles/Subsystems/datasheet/gs-ds-nanopower-dsp-11.pdf>. Accessed 12/05/2019.
- [75] ISISpace, *Solar Panels Brochure*. <https://www.isispace.nl/wp-content/uploads/2016/02/Solar-Panels-Brochure-v1.pdf>. Accessed 12/05/2019.
- [76] Andrews Space, *6U 20W Solar Panel*, 2015. <http://spaceflight.com/wp-content/uploads/2015/05/201410-6U-20W-Solar-Panel-Datasheet.pdf>. Accessed 12/05/2019.
- [77] DHV Technology, *Solar Panels for Aerospace Applications*, 2017. <http://dhvtechnology.com/wp-content/uploads/2017/05/DHV-Datasheet-Product-Space-Apr-17-web-1.pdf>. Accessed 12/05/2019.
- [78] DHV Technology, *6U & 12U Solar Panels*, 2017. <http://dhvtechnology.com/wp-content/uploads/2017/07/Datasheet-6U-Julio-v1-front-back.pdf>. Accessed 12/05/2019.

- [79] Cube Space, *CubeComputer V4.1*. <https://www.cubesatshop.com/wp-content/uploads/2016/06/CubeComputer-V4.1-Datasheet-v1.3.pdf>. Accessed 26/03/2019.
- [80] EnduroSat, *Onboard Computer (OBC)*. https://www.endurosat.com/modules-datasheets/OBC_User_Manual_Rev1.pdf. Accessed 26/03/2019.
- [81] GOMSpace, *NanoMind A3200*. <https://gomspace.com/UserFiles/Subsystems/datasheet/gs-ds-nanomind-a3200-114.pdf>. Accessed 26/03/2019.
- [82] EnduroSat, *Structure 6U*, 2019. https://cdn6.endurosat.com/modules-datasheets/STRT_6U_User_Manual_Rev1.2.pdf. Accessed 25/05/2019.
- [83] GOMSpace, *NanoStructure 6U*, 2018. <https://gomspace.com/UserFiles/Subsystems/datasheet/gs-ds-nanostructure-6u-11.pdf>. Accessed 25/05/2019.
- [84] Clydespace, *CPUT X-Band transmitter*. <https://satsearch.co/products/clyde-space-cput-x-band-transmitter>. Accessed 16/03/2019.
- [85] IQ SpaceCom, *X Band Transceiver SDR for Small Satellites*. <https://www.iq-spacecom.com/images/downloads/XLINK-Datasheet.pdf>. Accessed 16/03/2019.
- [86] Syrlinks, “EWC27 X Band Transmitter.” <https://www.syrlinks.com/en/space/nano-satellite/x-band-transmitter-ewc27>. Accessed 16/03/2019.
- [87] GOMSpace, *NanoPower P60*. <https://gomspace.com/UserFiles/Subsystems/datasheet/gs-ds-nanopower-p60-dock-29.pdf>. Accessed 18/03/2019.
- [88] EnduroSat, *1.5U Solar Panel*. https://cdn5.endurosat.com/modules-datasheets/Solar-Panel_1_5U-User_Manual_Rev1_1.pdf. Accessed 12/05/2019.

Appendix A

Orbit lifetime simulation results

This appendix contains color-coded tables with the STELA simulation results for orbit lifetime. In the tables, green indicates that the value is inside the 4 months to 25 years acceptable range, while red indicates that the value is outside.

Mean solar activity

	ISS 400km	SSO 400km	SSO 500km	SSO 600km	SSO 700km
Config. 1	1.05	1.06	5.87	28.08	110.89
Config. 3	0.75	0.75	4.03	18.98	76.3
Config. 4	0.53	0.54	2.92	13.59	55.25
Config. 5	0.56	0.56	3.03	14.12	57.33
Config. 6	0.5	0.51	2.79	12.9	52.66
Config. 7	0.39	0.39	2.19	10.13	41.12

Table A.0.1: Orbit lifetime for mean solar activity (150 sfu).

Maximum solar activity

	ISS 400km	SSO 400km	SSO 500km	SSO 600km	SSO 700km
Config. 1	0.55	0.57	2.49	9.62	33.77
Config. 3	0.38	0.38	1.77	6.47	23.76
Config. 4	0.28	0.28	1.28	4.94	17.06
Config. 5	0.29	0.29	1.33	5.13	17.73
Config. 6	0.27	0.27	1.23	4.73	16.23
Config. 7	0.22	0.22	0.98	3.76	12.91

Table A.0.2: Orbit lifetime for maximum solar activity (210 sfu).

Minimum solar activity

	ISS 400km	SSO 400km	SSO 500km	SSO 600km	SSO 700km
Config. 1	3.37	3.32	26.48	152.07	621.22
Config. 3	2.32	2.32	18.5	106.69	435.65
Config. 4	1.77	1.74	13.5	78.81	321.04
Config. 5	1.83	1.79	14.01	81.66	333.08
Config. 6	1.7	1.65	12.87	75.25	306.15
Config. 7	1.32	1.3	10.22	59.96	244.29

Table A.0.3: Orbit lifetime for minimum solar activity (75 sfu).

Appendix B

Battery power simulation results

This appendix contains the results of the simulations performed to assess the battery levels along each operational scenario proposed in Section 3.5.

The results for generic 10W, 20W, 30W and 40W payloads are presented. These have been used to determine the requirements for minimum battery capacity in each orbit, configuration and scenario.

Config.	BAT (Wh)	Mode 4 (W)	Eclipse (h)	BAT (Wh)	BAT (%)	Mode 1 (W)	Illum. (h)	BAT (Wh)	BAT (%)
ISS Orbit									
1	3.57	-2.950	0.604	1.789	50.099	7.550	0.937	3.570	100.000
2	3.57	-2.950	0.604	1.789	50.099	9.630	0.937	3.570	100.000
3	3.57	-2.950	0.604	1.789	50.099	20.990	0.937	3.570	100.000
4	3.57	-2.950	0.604	1.789	50.099	24.990	0.937	3.570	100.000
5	3.57	-2.950	0.604	1.789	50.099	27.870	0.937	3.570	100.000
6	3.57	-2.950	0.604	1.789	50.099	31.710	0.937	3.570	100.000
7	3.57	-2.950	0.604	1.789	50.099	34.590	0.937	3.570	100.000
8	3.57	-2.950	0.604	1.789	50.099	49.790	0.937	3.570	100.000
400 km SSO									
1	3.56	-2.950	0.603	1.783	50.074	7.550	0.940	3.560	100.000
2	3.56	-2.950	0.603	1.783	50.074	9.630	0.940	3.560	100.000
3	3.56	-2.950	0.603	1.783	50.074	20.990	0.940	3.560	100.000
4	3.56	-2.950	0.603	1.783	50.074	24.990	0.940	3.560	100.000
5	3.56	-2.950	0.603	1.783	50.074	27.870	0.940	3.560	100.000
6	3.56	-2.950	0.603	1.783	50.074	31.710	0.940	3.560	100.000
7	3.56	-2.950	0.603	1.783	50.074	34.590	0.940	3.560	100.000
8	3.56	-2.950	0.603	1.783	50.074	49.790	0.940	3.560	100.000

Table B.0.1: Scenario 1 for 10 W payload. ISS orbit and 400km SSO.

Config.	BAT (Wh)	Mode 4 (W)	Eclipse (h)	BAT (Wh)	BAT (%)	Mode 1 (W)	Illum. (h)	BAT (Wh)	BAT (%)
500 km SSO									
1	3.53	-2.950	0.597	1.770	50.137	7.550	0.980	3.530	100.000
2	3.53	-2.950	0.597	1.770	50.137	9.630	0.980	3.530	100.000
3	3.53	-2.950	0.597	1.770	50.137	20.990	0.980	3.530	100.000
4	3.53	-2.950	0.597	1.770	50.137	24.990	0.980	3.530	100.000
5	3.53	-2.950	0.597	1.770	50.137	27.870	0.980	3.530	100.000
6	3.53	-2.950	0.597	1.770	50.137	31.710	0.980	3.530	100.000
7	3.53	-2.950	0.597	1.770	50.137	34.590	0.980	3.530	100.000
8	3.53	-2.950	0.597	1.770	50.137	49.790	0.980	3.530	100.000
600 km SSO									
1	3.50	-2.950	0.592	1.753	50.084	7.550	1.019	3.500	100.000
2	3.50	-2.950	0.592	1.753	50.084	9.630	1.019	3.500	100.000
3	3.50	-2.950	0.592	1.753	50.084	20.990	1.019	3.500	100.000
4	3.50	-2.950	0.592	1.753	50.084	24.990	1.019	3.500	100.000
5	3.50	-2.950	0.592	1.753	50.084	27.870	1.019	3.500	100.000
6	3.50	-2.950	0.592	1.753	50.084	31.710	1.019	3.500	100.000
7	3.50	-2.950	0.592	1.753	50.084	34.590	1.019	3.500	100.000
8	3.50	-2.950	0.592	1.753	50.084	49.790	1.019	3.500	100.000

Table B.0.2: Scenario 1 for 10 W payload. 500km SSO and 600km SSO.

Config.	BAT (Wh)	Mode 2 (W)	COMM (h)	BAT (Wh)	BAT (%)	Mode 4 (W)	Eclipse (h)	BAT (Wh)	BAT (%)	Mode 1 (W)	Illum. (h)	BAT (%)
ISS Orbit												
1	5.19	-6.078	0.133	4.380	84.385	-2.950	0.604	2.598	50.060	7.550	0.804	100.000
2	3.57	2.090	0.133	3.570	100.000	-2.950	0.604	1.789	50.099	9.630	0.804	100.000
3	3.57	2.490	0.133	3.570	100.000	-2.950	0.604	1.789	50.099	20.990	0.804	100.000
4	3.57	15.362	0.133	3.570	100.000	-2.950	0.604	1.789	50.099	24.990	0.804	100.000
5	3.57	7.122	0.133	3.570	100.000	-2.950	0.604	1.789	50.099	27.870	0.804	100.000
6	3.57	9.602	0.133	3.570	100.000	-2.950	0.604	1.789	50.099	31.710	0.804	100.000
7	3.57	11.194	0.133	3.570	100.000	-2.950	0.604	1.789	50.099	34.590	0.804	100.000
8	3.57	21.882	0.133	3.570	100.000	-2.950	0.604	1.789	50.099	49.790	0.804	100.000
400 km SSO												
1	4.98	-6.078	0.117	4.271	85.761	-2.950	0.603	2.494	50.071	7.550	0.823	100.000
2	3.56	2.090	0.117	3.560	100.000	-2.950	0.603	1.783	50.074	9.630	0.823	100.000
3	3.56	2.490	0.117	3.560	100.000	-2.950	0.603	1.783	50.074	20.990	0.823	100.000
4	3.56	15.362	0.117	3.560	100.000	-2.950	0.603	1.783	50.074	24.990	0.823	100.000
5	3.56	7.122	0.117	3.560	100.000	-2.950	0.603	1.783	50.074	27.870	0.823	100.000
6	3.56	9.602	0.117	3.560	100.000	-2.950	0.603	1.783	50.074	31.710	0.823	100.000
7	3.56	11.194	0.117	3.560	100.000	-2.950	0.603	1.783	50.074	34.590	0.823	100.000
8	3.56	21.882	0.117	3.560	100.000	-2.950	0.603	1.783	50.074	49.790	0.823	100.000

Table B.0.3: Scenario 2 for 10 W payload. ISS orbit and 400km SSO.

Config.	BAT (Wh)	Mode 2 (W)	COMM (h)	BAT (Wh)	BAT (%)	Mode 4 (W)	Eclipse (h)	BAT (Wh)	BAT (%)	Mode 1 (W)	Illum. (h)	BAT (%)
500 km SSO												
1	5.15	-6.078	0.133	4.340	84.264	-2.950	0.597	2.579	50.086	7.550	0.847	100.000
2	3.53	2.090	0.133	3.530	100.000	-2.950	0.597	1.770	50.137	9.630	0.847	100.000
3	3.53	2.490	0.133	3.530	100.000	-2.950	0.597	1.770	50.137	20.990	0.847	100.000
4	3.53	15.362	0.133	3.530	100.000	-2.950	0.597	1.770	50.137	24.990	0.847	100.000
5	3.53	7.122	0.133	3.530	100.000	-2.950	0.597	1.770	50.137	27.870	0.847	100.000
6	3.53	9.602	0.133	3.530	100.000	-2.950	0.597	1.770	50.137	31.710	0.847	100.000
7	3.53	11.194	0.133	3.530	100.000	-2.950	0.597	1.770	50.137	34.590	0.847	100.000
8	3.53	21.882	0.133	3.530	100.000	-2.950	0.597	1.770	50.137	49.790	0.847	100.000
600 km SSO												
1	5.32	-6.078	0.150	4.408	82.863	-2.950	0.592	2.661	50.023	7.550	0.869	100.000
2	3.50	2.090	0.150	3.500	100.000	-2.950	0.592	1.753	50.084	9.630	0.869	100.000
3	3.50	2.490	0.150	3.500	100.000	-2.950	0.592	1.753	50.084	20.990	0.869	100.000
4	3.50	15.362	0.150	3.500	100.000	-2.950	0.592	1.753	50.084	24.990	0.869	100.000
5	3.50	7.122	0.150	3.500	100.000	-2.950	0.592	1.753	50.084	27.870	0.869	100.000
6	3.50	9.602	0.150	3.500	100.000	-2.950	0.592	1.753	50.084	31.710	0.869	100.000
7	3.50	11.194	0.150	3.500	100.000	-2.950	0.592	1.753	50.084	34.590	0.869	100.000
8	3.50	21.882	0.150	3.500	100.000	-2.950	0.592	1.753	50.084	49.790	0.869	100.000

Table B.0.4: Scenario 2 for 10 W payload. 500km SSO and 600km SSO.

Config.	BAT (Wh)	Mode 4 (W)	Eclipse (h)	BAT (Wh)	BAT (%)	Mode 2 (W)	COMM (h)	BAT (Wh)	BAT (%)	Mode 1 (W)	Illum. (h)	BAT (%)
ISS Orbit												
1	6.71	-2.950	0.471	5.322	79.312	-14.750	0.133	3.355	50.003	7.550	0.937	100.000
2	6.71	-2.950	0.471	5.322	79.312	-14.750	0.133	3.355	50.003	9.630	0.937	100.000
3	6.71	-2.950	0.471	5.322	79.312	-14.750	0.133	3.355	50.003	20.990	0.937	100.000
4	6.71	-2.950	0.471	5.322	79.312	-14.750	0.133	3.355	50.003	24.990	0.937	100.000
5	6.71	-2.950	0.471	5.322	79.312	-14.750	0.133	3.355	50.003	27.870	0.937	100.000
6	6.71	-2.950	0.471	5.322	79.312	-14.750	0.133	3.355	50.003	31.710	0.937	100.000
7	6.71	-2.950	0.471	5.322	79.312	-14.750	0.133	3.355	50.003	34.590	0.937	100.000
8	6.71	-2.950	0.471	5.322	79.312	-14.750	0.133	3.355	50.003	49.790	0.937	100.000
400 km SSO												
1	6.31	-2.950	0.486	4.877	77.287	-14.750	0.117	3.156	50.015	7.550	0.940	100.000
2	6.31	-2.950	0.486	4.877	77.287	-14.750	0.117	3.156	50.015	9.630	0.940	100.000
3	6.31	-2.950	0.486	4.877	77.287	-14.750	0.117	3.156	50.015	20.990	0.940	100.000
4	6.31	-2.950	0.486	4.877	77.287	-14.750	0.117	3.156	50.015	24.990	0.940	100.000
5	6.31	-2.950	0.486	4.877	77.287	-14.750	0.117	3.156	50.015	27.870	0.940	100.000
6	6.31	-2.950	0.486	4.877	77.287	-14.750	0.117	3.156	50.015	31.710	0.940	100.000
7	6.31	-2.950	0.486	4.877	77.287	-14.750	0.117	3.156	50.015	34.590	0.940	100.000
8	6.31	-2.950	0.486	4.877	77.287	-14.750	0.117	3.156	50.015	49.790	0.940	100.000

Table B.0.5: Scenario 3 for 10 W payload. ISS orbit and 400km SSO.

Config.	BAT (Wh)	Mode 4 (W)	Eclipse (h)	BAT (Wh)	BAT (%)	Mode 2 (W)	COMM (h)	BAT (Wh)	BAT (%)	Mode 1 (W)	Illum. (h)	BAT (%)
500km SSO												
1	6.67	-2.950	0.463	5.303	79.508	-14.750	0.133	3.337	50.022	7.550	0.980	100.000
2	6.67	-2.950	0.463	5.303	79.508	-14.750	0.133	3.337	50.022	9.630	0.980	100.000
3	6.67	-2.950	0.463	5.303	79.508	-14.750	0.133	3.337	50.022	20.990	0.980	100.000
4	6.67	-2.950	0.463	5.303	79.508	-14.750	0.133	3.337	50.022	24.990	0.980	100.000
5	6.67	-2.950	0.463	5.303	79.508	-14.750	0.133	3.337	50.022	27.870	0.980	100.000
6	6.67	-2.950	0.463	5.303	79.508	-14.750	0.133	3.337	50.022	31.710	0.980	100.000
7	6.67	-2.950	0.463	5.303	79.508	-14.750	0.133	3.337	50.022	34.590	0.980	100.000
8	6.67	-2.950	0.463	5.303	79.508	-14.750	0.133	3.337	50.022	49.790	0.980	100.000
600 km SSO												
1	7.04	-2.950	0.442	5.735	81.469	-14.750	0.150	3.523	50.042	7.550	1.019	100.000
2	7.04	-2.950	0.442	5.735	81.469	-14.750	0.150	3.523	50.042	9.630	1.019	100.000
3	7.04	-2.950	0.442	5.735	81.469	-14.750	0.150	3.523	50.042	20.990	1.019	100.000
4	7.04	-2.950	0.442	5.735	81.469	-14.750	0.150	3.523	50.042	24.990	1.019	100.000
5	7.04	-2.950	0.442	5.735	81.469	-14.750	0.150	3.523	50.042	27.870	1.019	100.000
6	7.04	-2.950	0.442	5.735	81.469	-14.750	0.150	3.523	50.042	31.710	1.019	100.000
7	7.04	-2.950	0.442	5.735	81.469	-14.750	0.150	3.523	50.042	34.590	1.019	100.000
8	7.04	-2.950	0.442	5.735	81.469	-14.750	0.150	3.523	50.042	49.790	1.019	100.000

Table B.0.6: Scenario 3 for 10 W payload. 500km SSO and 600km SSO.

Config.	BAT (Wh)	Mode 3 (W)	Acq. (h)	BAT (Wh)	BAT (%)	Mode 4 (W)	Eclipse (h)	BAT (Wh)	BAT (%)	Mode 1 (W)	Illum. (h)	BAT (%)
ISS Orbit												
1	5.7	-6.378	0.167	4.637	81.351	-2.950	0.604	2.856	50.097	3.750	0.770	100.000
2	3.57	1.790	0.167	3.570	100.000	-2.950	0.604	1.789	50.099	2.330	0.770	100.000
3	3.57	2.190	0.167	3.570	100.000	-2.950	0.604	1.789	50.099	11.990	0.770	100.000
4	3.57	15.062	0.167	3.570	100.000	-2.950	0.604	1.789	50.099	24.990	0.770	100.000
5	3.57	6.822	0.167	3.570	100.000	-2.950	0.604	1.789	50.099	27.870	0.770	100.000
6	3.57	9.302	0.167	3.570	100.000	-2.950	0.604	1.789	50.099	31.710	0.770	100.000
7	3.57	10.894	0.167	3.570	100.000	-2.950	0.604	1.789	50.099	34.590	0.770	100.000
8	3.57	21.582	0.167	3.570	100.000	-2.950	0.604	1.789	50.099	49.790	0.770	100.000
400 km SSO												
1	5.69	-6.378	0.167	4.627	81.318	-2.950	0.603	2.850	50.081	7.550	0.773	100.000
2	3.56	1.790	0.167	3.560	100.000	-2.950	0.603	1.783	50.074	9.630	0.773	100.000
3	3.56	2.190	0.167	3.560	100.000	-2.950	0.603	1.783	50.074	20.990	0.773	100.000
4	3.56	15.062	0.167	3.560	100.000	-2.950	0.603	1.783	50.074	24.990	0.773	100.000
5	3.56	6.822	0.167	3.560	100.000	-2.950	0.603	1.783	50.074	27.870	0.773	100.000
6	3.56	9.302	0.167	3.560	100.000	-2.950	0.603	1.783	50.074	31.710	0.773	100.000
7	3.56	10.894	0.167	3.560	100.000	-2.950	0.603	1.783	50.074	34.590	0.773	100.000
8	3.56	21.582	0.167	3.560	100.000	-2.950	0.603	1.783	50.074	49.790	0.773	100.000

Table B.0.7: Scenario 4 for 10 W payload. ISS orbit and 400km SSO.

Config.	BAT (Wh)	Mode 3 (W)	Acq. (h)	BAT (Wh)	BAT (%)	Mode 4 (W)	Eclipse (h)	BAT (Wh)	BAT (%)	Mode 1 (W)	Illum. (h)	BAT (%)
500km SSO												
1	5.65	-6.378	0.167	4.587	81.186	-2.950	0.597	2.827	50.032	7.550	0.813	100.000
2	3.53	1.790	0.167	3.530	100.000	-2.950	0.597	1.770	50.137	9.630	0.813	100.000
3	3.53	2.190	0.167	3.530	100.000	-2.950	0.597	1.770	50.137	20.990	0.813	100.000
4	3.53	15.062	0.167	3.530	100.000	-2.950	0.597	1.770	50.137	24.990	0.813	100.000
5	3.53	6.822	0.167	3.530	100.000	-2.950	0.597	1.770	50.137	27.870	0.813	100.000
6	3.53	9.302	0.167	3.530	100.000	-2.950	0.597	1.770	50.137	31.710	0.813	100.000
7	3.53	10.894	0.167	3.530	100.000	-2.950	0.597	1.770	50.137	34.590	0.813	100.000
8	3.53	21.582	0.167	3.530	100.000	-2.950	0.597	1.770	50.137	49.790	0.813	100.000
600 km SSO												
1	5.63	-6.378	0.167	4.567	81.119	-2.950	0.592	2.820	50.088	7.550	0.853	100.000
2	3.5	1.790	0.167	3.500	100.000	-2.950	0.592	1.753	50.084	9.630	0.853	100.000
3	3.5	2.190	0.167	3.500	100.000	-2.950	0.592	1.753	50.084	20.990	0.853	100.000
4	3.5	15.062	0.167	3.500	100.000	-2.950	0.592	1.753	50.084	24.990	0.853	100.000
5	3.5	6.822	0.167	3.500	100.000	-2.950	0.592	1.753	50.084	27.870	0.853	100.000
6	3.5	9.302	0.167	3.500	100.000	-2.950	0.592	1.753	50.084	31.710	0.853	100.000
7	3.5	10.894	0.167	3.500	100.000	-2.950	0.592	1.753	50.084	34.590	0.853	100.000
8	3.5	21.582	0.167	3.500	100.000	-2.950	0.592	1.753	50.084	49.790	0.853	100.000

Table B.0.8: Scenario 4 for 10 W payload. 500km SSO and 600km SSO.

Config.	BAT (Wh)	Mode 3 (W)	Acq. (h)	BAT (Wh)	BAT (%)	Mode 4 (W)	Eclipse (h)	BAT (Wh)	BAT (%)	Mode 1 (W)	Illum. (h)	BAT (%)
ISS Orbit												
1	9.03	-16.378	0.167	6.300	69.771	-2.950	0.604	4.519	50.043	5.850	0.770	100.000
2	6.3	-8.210	0.167	4.932	78.280	-2.950	0.604	3.150	50.003	4.130	0.770	100.000
3	6.17	-7.810	0.167	4.868	78.903	-2.950	0.604	3.087	50.030	4.090	0.770	100.000
4	3.57	5.062	0.167	3.57	100.000	-2.950	0.604	1.789	50.099	5.990	0.770	100.000
5	4.63	-3.178	0.167	4.100	88.560	-2.950	0.604	2.319	50.083	8.870	0.770	100.000
6	3.8	-0.698	0.167	3.684	96.939	-2.950	0.604	1.902	50.058	12.710	0.770	100.000
7	3.57	0.894	0.167	3.57	100.000	-2.950	0.604	1.789	50.099	34.590	0.770	100.000
8	3.57	11.582	0.167	3.57	100.000	-2.950	0.604	1.789	50.099	49.790	0.770	100.000
400 km SSO												
1	9.02	-16.378	0.167	6.290	69.738	-2.950	0.603	4.513	50.033	7.550	0.773	100.000
2	6.3	-8.210	0.167	4.932	78.280	-2.950	0.603	3.154	50.068	9.630	0.773	100.000
3	6.16	-7.810	0.167	4.858	78.869	-2.950	0.603	3.081	50.016	20.990	0.773	100.000
4	3.56	5.062	0.167	3.56	100.000	-2.950	0.603	1.783	50.074	24.990	0.773	100.000
5	4.62	-3.178	0.167	4.090	88.535	-2.950	0.603	2.313	50.064	27.870	0.773	100.000
6	3.79	-0.698	0.167	3.674	96.931	-2.950	0.603	1.896	50.034	31.710	0.773	100.000
7	3.56	0.894	0.167	3.56	100.000	-2.950	0.603	1.783	50.074	34.590	0.773	100.000
8	3.56	11.582	0.167	3.56	100.000	-2.950	0.603	1.783	50.074	49.790	0.773	100.000

Table B.0.9: Scenario 4 for 20 W payload. ISS orbit and 400km SSO.

Config.	BAT (Wh)	Mode 3 (W)	Acq. (h)	BAT (Wh)	BAT (%)	Mode 4 (W)	Eclipse (h)	BAT (Wh)	BAT (%)	Mode 1 (W)	Illum. (h)	BAT (%)
500km SSO												
1	8.98	-16.378	0.167	6.250	69.603	-2.950	0.597	4.490	50.002	7.550	0.813	100.000
2	6.26	-8.210	0.167	4.892	78.142	-2.950	0.597	3.132	50.024	9.630	0.813	100.000
3	6.13	-7.810	0.167	4.828	78.766	-2.950	0.597	3.068	50.052	20.990	0.813	100.000
4	3.53	5.062	0.167	3.53	100.000	-2.950	0.597	1.770	50.137	24.990	0.813	100.000
5	4.58	-3.178	0.167	4.050	88.435	-2.950	0.597	2.290	50.004	27.870	0.813	100.000
6	3.76	-0.698	0.167	3.644	96.906	-2.950	0.597	1.884	50.093	31.710	0.813	100.000
7	3.53	0.894	0.167	3.53	100.000	-2.950	0.597	1.770	50.137	34.590	0.813	100.000
8	3.53	11.582	0.167	3.53	100.000	-2.950	0.597	1.770	50.137	49.790	0.813	100.000
600 km SSO												
1	8.96	-16.378	0.167	6.230	69.535	-2.950	0.592	4.483	50.037	7.550	0.853	100.000
2	6.24	-8.210	0.167	4.872	78.072	-2.950	0.592	3.125	50.074	9.630	0.853	100.000
3	6.1	-7.810	0.167	4.798	78.661	-2.950	0.592	3.051	50.021	20.990	0.853	100.000
4	3.5	5.062	0.167	3.5	100.000	-2.950	0.592	1.753	50.084	24.990	0.853	100.000
5	4.56	-3.178	0.167	4.030	88.385	-2.950	0.592	2.283	50.072	27.870	0.853	100.000
6	3.73	-0.698	0.167	3.614	96.881	-2.950	0.592	1.867	50.043	31.710	0.853	100.000
7	3.5	0.894	0.167	3.5	100.000	-2.950	0.592	1.753	50.084	34.590	0.853	100.000
8	3.5	11.582	0.167	3.5	100.000	-2.950	0.592	1.753	50.084	49.790	0.853	100.000

Table B.0.10: Scenario 4 for 20 W payload. 500km SSO and 600km SSO.

Config.	BAT (Wh)	Mode 3 (W)	Acq. (h)	BAT (Wh)	BAT (%)	Mode 4 (W)	Eclipse (h)	BAT (Wh)	BAT (%)	Mode 1 (W)	Illum. (h)	BAT (%)
30 W Payload, ISS Orbit												
1	12.36	-26.378	0.167	7.964	64.431	-2.950	0.604	6.182	50.018	8.050	0.770	100.000
2	9.64	-18.210	0.167	6.605	68.517	-2.950	0.604	4.824	50.037	6.330	0.770	100.000
3	9.50	-17.810	0.167	6.532	68.754	-2.950	0.604	4.750	50.002	6.090	0.770	100.000
4	5.21	-4.938	0.167	4.387	84.203	-2.950	0.604	2.606	50.010	3.290	0.770	100.000
5	7.96	-13.178	0.167	5.764	72.408	-2.950	0.604	3.982	50.028	5.170	0.770	100.000
6	7.13	-10.698	0.167	5.347	74.993	-2.950	0.604	3.566	50.007	4.610	0.770	100.000
7	6.60	-9.106	0.167	5.082	77.005	-2.950	0.604	3.301	50.013	5.590	0.770	100.000
8	3.57	1.582	0.167	3.570	100.000	-2.950	0.604	1.789	50.099	20.790	0.770	100.000
40 W Payload, ISS Orbit												
1	15.69	-36.378	0.167	9.627	61.358	-2.950	0.604	7.846	50.003	8.550	0.770	100.000
2	12.97	-28.210	0.167	8.268	63.750	-2.950	0.604	6.487	50.014	8.430	0.770	100.000
3	12.84	-27.810	0.167	8.205	63.902	-2.950	0.604	6.424	50.027	8.290	0.770	100.000
4	8.55	-14.938	0.167	6.060	70.881	-2.950	0.604	4.279	50.045	5.590	0.770	100.000
5	11.29	-23.178	0.167	7.427	65.784	-2.950	0.604	5.646	50.005	7.270	0.770	100.000
6	10.47	-20.698	0.167	7.020	67.052	-2.950	0.604	5.239	50.037	6.810	0.770	100.000
7	9.94	-19.106	0.167	6.756	67.964	-2.950	0.604	4.974	50.042	6.390	0.770	100.000
8	6.37	-8.418	0.167	4.967	77.975	-2.950	0.604	3.186	50.008	10.790	0.770	100.000

Table B.0.11: Scenario 4 for 30 W and 40 W payload. ISS orbit.